agronomy

MDPI

Article

Optimizing Total Nitrogen Rate and Starter Nitrogen Proportion for Spring Maize Under Shallow-Buried Drip Irrigation Using a Sensitivity-Calibrated DNDC Model

Yongqiang Wang [1,2,*], Jinfeng Liu [1], Lidong Han [1] and Fugui Wang [1,2,*]

1 College of Agronomy, Inner Mongolia Agricultural University, Hohhot 010018, China; 18371915622@163.com (J.L.); 15539349611@163.com (L.H.)
2 Inner Mongolia Autonomous Region Industrial Technology Engineering Center for Intelligent Water and Fertilizer Management Technology and Equipment for Crops, Hohhot 010018, China
* Correspondence: yqwang@imau.edu.cn (Y.W.); nmgwfg@imau.edu.cn (F.W.)

Abstract

Optimizing nitrogen management is essential for maintaining high spring maize yield while mitigating nitrous oxide (N_2O) emissions in irrigated areas. However, the interactive effects of total nitrogen application rate and starter nitrogen proportion on yield and N_2O emissions remain insufficiently quantified. Reliable assessment of these interactions requires well-calibrated DeNitrification–DeComposition (DNDC) simulations, yet existing calibration studies often emphasize crop parameters while neglecting soil parameters critical for soil hydrothermal dynamics and N_2O production. In this study, field data from shallow-buried drip-irrigated spring maize in Tongliao during 2024–2025 were used to conduct Extended Fourier Amplitude Sensitivity Test (EFAST) sensitivity analysis on 12 crop and 13 soil parameters of the DNDC model. Sensitive parameters were calibrated using the differential evolution algorithm, and 64 nitrogen management scenarios were simulated by combining eight total nitrogen application rates (100, 150, 200, 250, 300, 350, 400, and 450 kg N ha^{-1}) with eight starter nitrogen proportions (0%, 15%, 25%, 30%, 35%, 40%, 45%, and 50% of the total nitrogen rate). The results showed that DNDC outputs were jointly controlled by crop and soil parameters, among which maximum yield, leaf carbon-to-nitrogen ratio, stem fraction, grain carbon-to-nitrogen ratio, thermal degree days for maturity, grain fraction, soil organic carbon (SOC) decrease rate below topsoil, soil clay content, soil porosity, wilting point and depth of top soil with uniform SOC content were dominant. Compared with the conventional crop-parameter calibration, the sensitivity-screened parameter set improved the simulation of both cumulative N_2O emissions and yield. Across the 64 scenarios, cumulative N_2O emissions ranged from 0.42 to 4.87 kg [N]/ha, while simulated maize yield ranged from 1597 to 6347 kg [C]/ha. N_2O emissions increased with total nitrogen rate, whereas yield increased initially and then reached a plateau. Increasing the starter nitrogen proportion did not substantially enhance yield but increased N_2O emission risk under high nitrogen rates. Overall, the scenario with 300 kg/ha and no nitrogen applied at sowing achieved a relatively high yield of 5519 kg [C]/ha while maintaining a low cumulative N_2O emission of 0.98 kg [N]/ha and was therefore identified as the preferred trade-off strategy under shallow-buried drip irrigation. This study provides an EFAST–DNDC framework for optimizing nitrogen management to sustain spring maize yield while reducing N_2O emissions in the West Liaohe Plain.

Check for updates

Received: 14 May 2026
Revised: 4 June 2026
Accepted: 16 June 2026
Published: 18 June 2026

Copyright: © 2026 by the authors. Licensee MDPI, Basel, Switzerland. This article is an open access article distributed under the terms and conditions of the Creative Commons Attribution (CC BY) license.

 https://doi.org/10.3390/agronomy16121192

Keywords: corn; DNDC model; sensitivity analysis; model calibration; nitrogen management

1. Introduction

Against the background of global climate change and the green, low-carbon transformation of agriculture, reducing greenhouse gas emissions from croplands while maintaining grain yield has become a critical scientific issue in the optimization of crop production systems. Nitrous oxide (N_2O) is an important greenhouse gas emitted from agroecosystems [1]. N_2O emissions from agricultural soils are closely linked to nitrogen fertilizer management, particularly the amount, timing, and placement of nitrogen application [2]. Maize is a typical crop with a high nitrogen demand, and inappropriate nitrogen application can intensify the risk of N_2O emissions from croplands [3,4]. Under shallow-buried drip irrigation and integrated water–fertilizer management, nitrogen management for spring maize involves not only differences in the total nitrogen application rate throughout the growing season, but also variations in the amount of nitrogen applied as starter fertilizer at sowing. Therefore, clarifying the effects of total nitrogen application rate and starter nitrogen rate on yield formation and N_2O emissions in spring maize is a prerequisite for identifying nitrogen management strategies that achieve both high yield and low emissions.

The irrigated area of the West Liaohe Plain is an important spring maize production region in northern China. This region has abundant light and heat resources but relatively limited precipitation; therefore, maize production relies heavily on irrigation and nitrogen fertilizer inputs. In recent years, shallow-buried drip irrigation combined with integrated water–fertilizer management has been gradually promoted in this region, providing favorable conditions for precise water and nitrogen supply as well as split nitrogen application [5]. Under this production system, nitrogen management is determined not only by the total nitrogen application rate, but also by the proportion of nitrogen applied as starter fertilizer at sowing. A higher starter nitrogen proportion may increase mineral nitrogen availability in the root zone during the seedling stage, but it may also cause excessive early-season nitrogen accumulation when crop nitrogen demand is still low, thereby increasing the risk of subsequent nitrogen losses and N_2O emissions [6]. Conversely, a lower starter nitrogen proportion may reduce early nitrogen supply intensity, but sufficient nitrogen topdressing at later growth stages may compensate for this reduction and avoid substantial yield loss [7]. Therefore, the yield and N_2O emission responses of spring maize cannot be fully explained by total nitrogen rate or starter nitrogen proportion alone. It is necessary to evaluate how different total nitrogen application rates interact with different starter nitrogen proportions to regulate nitrogen supply–demand matching, yield formation, and N_2O emissions.

However, systematically evaluating such interactions through field experiments alone is time-consuming, labor-intensive, and difficult to extend to a wide range of nitrogen management scenarios [8]. Process-based crop models can help overcome these limitations by integrating crop growth, soil hydrothermal dynamics, carbon and nitrogen cycling, and greenhouse gas emissions into a unified simulation framework [9]. Therefore, they provide effective tools for extending field observations, conducting scenario simulations, and quantitatively assessing the effects of alternative nitrogen management strategies on crop yield and N_2O emissions. Among these models, the DNDC (DeNitrification–DeComposition) model is a widely used process-based biogeochemical model that can comprehensively simulate crop growth, soil temperature and moisture, carbon and nitrogen cycling, and CO_2, CH_4, and N_2O emissions in agroecosystems [10–12]. It has been extensively applied across different regions and cropping systems to evaluate the effects of fertilization, irrigation, tillage, and other field management practices on crop yield and greenhouse gas emissions [13]. However, the DNDC model is a high-dimensional, nonlinear model with multiple interacting processes, and its simulation outputs are jointly affected by various types of parameters related to climate, soil properties, crop cultivars, and field management. Direct use of default parameters often fails to accurately represent the soil hydrothermal conditions, crop growth characteristics, and nitrogen transformation processes of a specific region. Therefore, before applying the DNDC model to regional assessments of crop production and greenhouse gas emissions, parameter sensitivity analysis and localized calibration are essential steps for improving model reliability.

The DNDC model is a process-based model characterized by complex interactions among multiple parameters [8]. Calibrating all parameters is not only computationally expensive but may also introduce equifinality problems, thereby reducing parameter robustness. Global sensitivity analysis can identify key parameters that dominate model output uncertainty within specified parameter ranges, while explicitly accounting for nonlinear effects and interactions among parameters [14]. It has therefore become an important preliminary step for parameter optimization in complex crop models. The Extended Fourier Amplitude Sensitivity Test (EFAST), as a global sensitivity analysis method, can simultaneously estimate first-order and total-order sensitivity indices with relatively high computational efficiency, making it particularly suitable for screening sensitive parameters in crop models [15]. Wang et al. [14] applied the EFAST method to conduct global sensitivity analysis of CERES-Maize parameters under different irrigation and fertilizer stress conditions. Their results further showed that, in addition to maize cultivar parameters, soil and management-related parameters became important under water-stress conditions. This study indicates that soil-related parameters, in addition to crop parameters, should be considered in parameter sensitivity analysis. However, for the DNDC model, studies that simultaneously conduct global sensitivity analysis of both crop and soil parameters remain limited.

For DNDC model calibration, crop-related parameters, such as maximum yield, biomass allocation fractions, carbon-to-nitrogen (C/N) ratios of different plant organs, and accumulated thermal time for maturity, are commonly adjusted because they directly influence phenological development, biomass accumulation, and yield simulation [16]. At the same time, previous DNDC studies have also demonstrated that soil physicochemical parameters, including soil texture, bulk density, porosity, hydraulic parameters, soil organic carbon, and initial mineral nitrogen, can strongly affect soil hydrothermal dynamics, nitrogen transformation, crop growth, and N_2O emissions [17]. Therefore, DNDC calibration should not be viewed as a crop-parameter-only procedure; instead, the relative importance of crop and soil parameters may vary with region, soil type, cropping system, irrigation regime, and nitrogen management practice. However, for shallow-buried drip-irrigated spring maize in the West Liaohe Plain, particularly in the Tongliao region, localized DNDC calibration studies that simultaneously screen and optimize both crop and soil parameters based on global sensitivity analysis remain limited. This gap is important because the intensive fertigation practices and variable starter nitrogen proportions in this area may alter the dominant controls on yield formation and N_2O emissions. Therefore, a sensitivity-based calibration strategy that jointly considers crop and soil parameters is needed to improve the reliability of DNDC simulations and subsequent nitrogen management scenario analysis in this region.

Therefore, this study focused on spring maize fields in the irrigated area of the West Liaohe Plain, Tongliao, Inner Mongolia. Based on field experimental data under different starter nitrogen rates, the EFAST method was used to conduct a global sensitivity analysis of crop and soil parameters in the DNDC model, and the differential evolution algorithm was then applied to calibrate the sensitive parameters. On this basis, scenario combinations of different total nitrogen application rates and starter nitrogen rates were constructed to evaluate their effects on spring maize yield and cumulative N_2O emissions. The specific objectives of this study were to: (1) determine whether the dominant sensitive parameters of the DNDC model for spring maize fields in Tongliao include both crop and soil parameters; (2) develop a calibrated parameter set suitable for the DNDC model in spring maize systems in the Tongliao region; and (3) propose an optimized nitrogen fertilizer management strategy that balances crop yield and N_2O emission mitigation. This study provides a methodological reference for the localized application of the DNDC model in spring maize systems in irrigated areas, and offers a scientific basis for optimizing nitrogen fertilizer management to coordinate high spring maize yield with greenhouse gas emission mitigation in the irrigated area of the West Liaohe Plain.

2. Materials and Methods

2.1. Overview of the Study Area

The field experiments were conducted from May to October in 2024 and 2025 at the Maize Science and Technology Backyard in Tongliao, Inner Mongolia Autonomous Region, China (122°43′ E, 43°37′ N; altitude: 180 m above sea level). The experimental area has a temperate continental monsoon climate, characterized by abundant solar radiation. The annual sunshine duration is approximately 2800–3000 h, the mean annual air temperature is 5–8 °C, the annual precipitation is approximately 280–390 mm, and the frost-free period lasts 150–170 days. Maize is usually sown in early May and harvested in early October. The geographical location of the study area is shown in Figure 1.

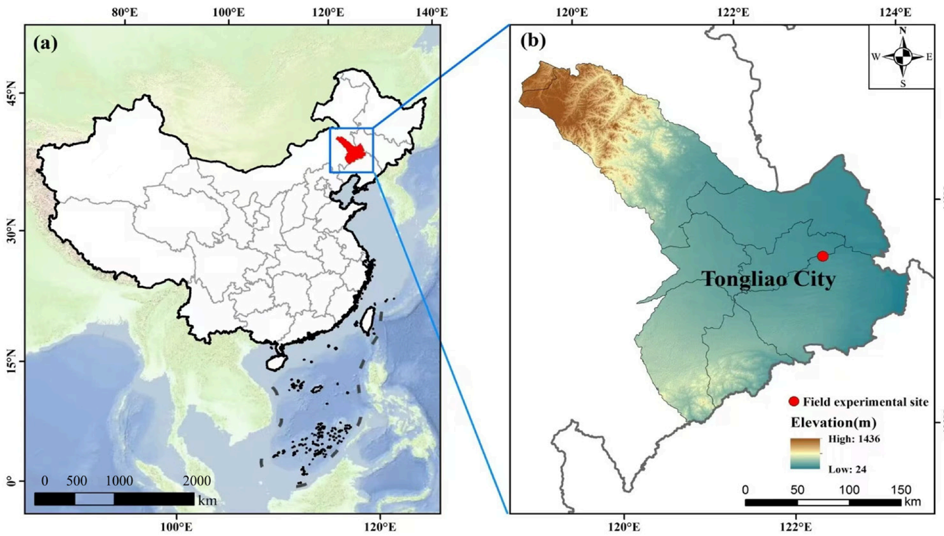

Figure 1. Geographical location of the experimental site. (**a**) Location of Tongliao City within China; (**b**) location of the field experimental site within Tongliao City, Inner Mongolia Autonomous Region, China.

2.2. Experimental Design

Three starter nitrogen application treatments were established, corresponding to 15% (N15), 30% (N30), and 45% (N45) of the total nitrogen application rate. Each treatment was replicated three times, resulting in a total of nine plots arranged in a randomized block design. Each plot covered an area of 11 m × 8 m, equivalent to 88 m^2. The mineral fertilizer rates were determined according to the programmed target yield of local high-yield spring maize production under shallow-buried drip irrigation. The total amounts of pure N, P_2O_5, and K_2O applied during the entire maize growing season were 300, 108, and 54 kg/ha, respectively. Urea (N $\geq$ 46%) was used as the nitrogen fertilizer, calcium superphosphate (P_2O_5 $\geq$ 16%) as the phosphorus fertilizer, and potassium sulfate (K_2O $\geq$ 52%) as the potassium fertilizer. All phosphorus and potassium fertilizers were applied as starter fertilizers at sowing by side-deep placement using a seeder.

Except for the nitrogen applied as starter fertilizer, the remaining nitrogen was fertigated with irrigation water at the jointing stage (V6), twelve-leaf stage (V12), silking stage (R1), and milk stage (R3) at a ratio of 2:5:2:1. This split ratio was selected based on the seasonal nitrogen demand pattern of spring maize and local fertigation practices under shallow-buried drip irrigation. A moderate nitrogen supply at V6 supports early vegetative growth, the largest proportion at V12 meets the high nitrogen demand during rapid biomass accumulation, and the smaller applications at R1 and R3 support reproductive growth and grain filling while reducing the risk of excessive late-season nitrogen accumulation. Irrigation was initiated for all treatments when the soil water content in the plough layer of any plot reached the lower irrigation threshold, which was set at 70% of field capacity during the seedling stage and 75% of field capacity during the other growth stages. The irrigation amount for each event was calculated as follows:

$$Q = U \times \rho \times (\theta_f - \theta_a) \times P/\partial \tag{1}$$

where Q is the irrigation amount per event (mm); U is the planned soil wetting depth at different maize growth stages, which was set to 30 cm at the seedling stage and 60 cm at the other growth stages; ρ is the soil bulk density of the planned wetting layer (g/cm^3); θ_f and θ_a are the soil field capacity and actual soil water content, respectively; P is the soil wetting ratio, which was set to 0.70; and ∂ is the irrigation water use efficiency under drip irrigation, which was set to 0.95 [18]. The irrigation amounts and nitrogen application rates at different growth stages are shown in Table 1.

Table 1. Irrigation and nitrogen application schedule during the whole maize growing season.

Treatment	Growth Stage									
	Sowing		V6		V12		R1		R3	
	Nitrogen Rate kg/ha	Irrigation mm	Nitrogen Rate kg/ha	Irrigation mm	Nitrogen Rate kg/ha	Irrigation mm	Nitrogen Rate kg/ha	Irrigation mm	Nitrogen Rate kg/ha	Irrigation mm
N15	45	28.8	51	72	127.5	72	51	72	25.5	72
N30	90	28.8	42	72	105	72	42	72	21	72
N45	135	28.8	33	72	82.5	72	33	72	16.5	72

Note: V6, V12, R1, and R3 refer to the six-leaf stage, twelve-leaf stage, silking stage, and milk stage, respectively.

Before sowing, the field was subjected to deep ploughing to a depth of 30 cm, followed by land leveling and seedbed preparation. The locally dominant maize cultivar Dika 159 was used in the experiment. Maize was planted in a wide–narrow row pattern, with narrow and wide row spacings of 40 and 80 cm, respectively, at a planting density of 90,000 plants/ha. This wide–narrow row pattern is the dominant local planting pattern for spring maize under shallow-buried drip irrigation in the Tongliao region and was therefore adopted to ensure consistency with local production practices. Irrigation was applied using a shallow-buried drip irrigation system without plastic film mulching. One drip irrigation tape was laid along the centerline of each narrow row, allowing precise irrigation of two adjacent maize rows with a single drip tape. In 2024, maize was sown on 4 May and harvested on 4 October. In 2025, maize was sown on 4 May and reached maturity on 6 October. The maize planting pattern and drip tape arrangement are shown in Figure 2.

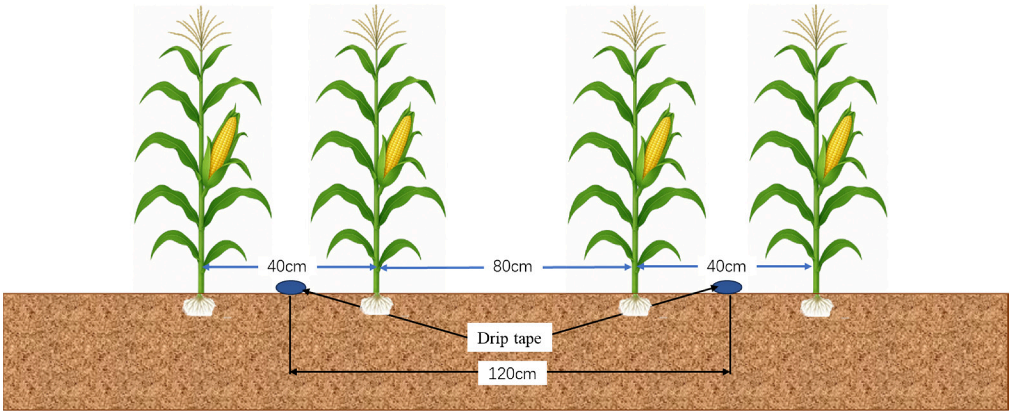

Figure 2. Schematic diagram of the wide–narrow row planting pattern and drip tape arrangement for maize.

2.3. Data Collection and Methods

2.3.1. Nitrous Oxide (N_2O)

N_2O emission fluxes were measured using the static chamber–gas chromatography method [19]. Each static chamber was used together with a base frame and had dimensions of 40 cm × 30 cm × 40 cm in length, width, and height, respectively. The outer surface of the chamber was wrapped with aluminum foil to minimize the influence of solar radiation on the air temperature inside the chamber. A thermometer was inserted through a rubber stopper at the top of the chamber, and a gas sampling port was installed on the sidewall and connected to a three-way valve. The valve was compatible with a 50 mL syringe, and all chamber interfaces were well sealed to ensure gas tightness. Gas sampling began after sowing and was conducted at the V6, V12, R1, and R3 stages. At each growth stage, gas samples were collected for five consecutive days. Sampling was conducted between 10:00 and 12:00 Beijing time, with gas samples collected every 10 min, resulting in four samples per sampling event. The N_2O emission flux was calculated using Equation (2) [16]:

$$F = \frac{M}{22.4} \times \frac{273}{273 + T} \times 60 \times H \times \frac{d_c}{d_t} \quad (2)$$

where F is the N_2O emission flux ($\mathrm{mg[N_2O]/m^2/h}$); H is the effective height of the sampling chamber, which was 0.4 m; M is the molar mass of N_2O, which was 44 g/mol; T is the air temperature inside the sampling chamber (°C); and d_c/d_t is the slope of the regression curve between N_2O concentration and sampling time. Cumulative N_2O emissions were calculated using Equation (3):

$$G_N = \sum_{i=1}^{n} \left(F_i \times d_i \times \frac{24}{100} \times \varepsilon \right) \quad (3)$$

where G_N is the total cumulative N_2O emission (kg[N]/ha); F_i is the N_2O emission flux at the ith sampling event ($\mathrm{mg/m^2/h}$); d_i is the interval between the ith sampling event and the subsequent sampling event (days); 100 is the unit conversion coefficient; ε is the mass fraction of N in N_2O (0.64).

2.3.2. Soil Temperature and Water Content

At the seedling, V6, V12, R1, and R3 stages, three sampling points were selected at equal intervals along the diagonal line of each plot. Soil temperature at 0–10 cm depth and volumetric soil water content at 0–10 cm depth were measured using a portable integrated soil temperature and moisture meter (FDS-200 series, Qingyi Electronic (Tianjin) Co., Ltd., Tianjin, China). Because soil water content in the DNDC model is expressed as water-filled pore space (*WFPS*) [20], volumetric soil water content was further converted to *WFPS* using the following equation:

$$WFPS = \frac{\theta_v}{1 - BD/\omega} \tag{4}$$

where *WFPS* is the soil water-filled pore space (cm^3/cm^3), θ_v is the volumetric soil water content (cm^3/cm^3), *BD* is the soil bulk density (g/cm^3), and ω is the mean soil particle density (g/cm^3), which was set to 2.65 g/cm^3. In this study, soil water content was expressed as WFPS.

2.3.3. Yield

At maize maturity, 20 consecutive plants were randomly selected from each experimental plot. After air drying, yield components, including ear number, grain number per ear, and 1000-grain weight, were measured, and grain dry matter yield was determined. To facilitate comparison with the simulated grain carbon content from the DNDC model (kg[C]/ha), the measured grain yield was converted into carbon content using the following equation:

$$Y_c = Y_{dry} \times \beta \tag{5}$$

where Y_c is the grain carbon content (kg[C]/ha), Y_{dry} is the grain yield on a dry matter basis (kg/ha), and β is the conversion coefficient between yield and carbon content, typically taken as 0.45 [21]. Therefore, the yield values reported for model calibration, validation, and scenario simulation are expressed as kg [C]/ha.

2.4. Sensitivity Analysis of DNDC Model Parameters

2.4.1. Overview of the DNDC Model

In this study, the DNDC model (Version 9.5) was used to simulate maize growth. The main model input parameters included meteorological data, soil data, crop parameters, and field management data.

(1) Meteorological data: Daily precipitation (mm), daily maximum air temperature (°C), and daily minimum air temperature (°C) during 2024–2025 were obtained from an automatic weather station installed at the Science and Technology Backyard. The temporal dynamics of daily minimum temperature, maximum temperature, and precipitation during the maize growing season are shown in Figure 3.

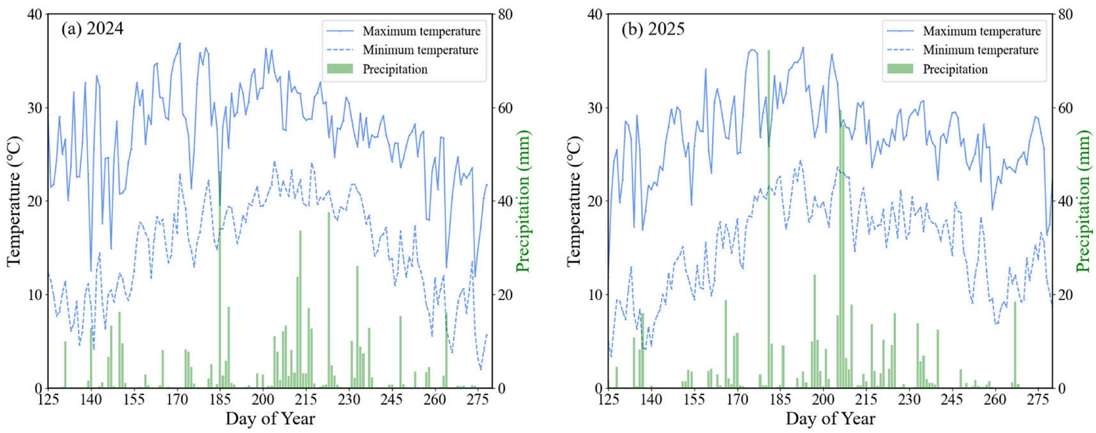

Figure 3. Daily maximum temperature, minimum temperature, and precipitation during the maize growing seasons in 2024 (**a**) and 2025 (**b**) at the experimental station.

(2) Soil data: Soil samples were collected before sowing from the 0–80 cm soil profile to characterize the root-zone soil hydraulic conditions of maize. Although the DNDC model requires surface soil hydraulic parameters for the 0–10 cm layer as model input, the measured soil hydraulic properties for the 0–80 cm profile are provided in Table 2 to more fully describe the soil conditions for maize growth. Soil texture was determined using a laser particle size analyzer [22], soil bulk density was measured using the cutting ring method [23], and soil pH was measured using a pH meter. Saturated water content, field capacity, and wilting point were estimated using soil water characteristic software. The soil properties are presented in Table 2.

Table 2. Soil properties at the experimental station.

Soil Layer (cm)	Soil Texture	pH	Bulk Density (g/cm^3)	Wilting Point (cm^3/cm^3)	Field Capacity (cm^3/cm^3)	Saturated Water Content (cm^3/cm^3)
0–10	Sandy soil	8.1	1.60	0.098	0.165	0.384
10–20		8.1	1.62	0.098	0.166	0.385
20–40		8.0	1.66	0.107	0.174	0.394
40–60		8.0	1.68	0.101	0.169	0.382
60–80		8.0	1.70	0.105	0.170	0.380

(3) Crop parameters: The crop parameters in the DNDC model mainly consist of cultivar-specific parameters. These parameters include grain fraction, leaf fraction, stem fraction, accumulated thermal time, and other cultivar-related traits. Owing to differences in genetic background among cultivars, these parameter values vary among maize varieties, thereby directly affecting the model accuracy in simulating crop growth dynamics, predicting yield, and representing coupled carbon–nitrogen cycling. The crop parameters are listed in Table 3.

(4) Field management data: Field management parameters mainly represented management practices related to planting information, including sowing date, sowing depth, and planting pattern; irrigation information, including irrigation date, irrigation amount, and irrigation method; and fertilization information, including fertilization date, fertilizer application rate, and fertilization method.

Table 3. Crop parameters and soil parameters for the 0–10 cm soil depth used in the DNDC model.

Parameters Type	Description	Acronym	Unit	Min	Max
crop parameters	Maximum yield	MYIELD	kg C/ha	2940	5460
	Grain fraction	GF	-	0.30	0.55
	Leaf fraction	LF	-	0.14	0.26
	Stem fraction	SF	-	0.14	0.26
	Grain C/N ratio	GCN	-	25	80
	Leaf C/N ratio	LCN	-	35	80
	Stem C/N ratio	SCN	-	35	80
	Root C/N ratio	RCN	-	35	80
	Thermal degree days for maturity	THERD	°C	1785	3315
	Water demand	WATD	g water/g DM	130	325
	Nitrogen fixation index	NFIX	crop N/N soil	0	1
	Optimum temperature	OPTTEM	°C	21	35

https://doi.org/10.3390/agronomy16121192

Table 3. *Cont.*

Parameters Type	Description	Acronym	Unit	Min	Max
soil parameters	Soil clay content	CLAY	-	0.03	0.63
	Soil bulk density	BD	g/cm^3	0.50	2.25
	Field capacity	FC	cm^3/cm^3	0	1.00
	Wilting point	WILP	cm^3/cm^3	0	1.00
	Saturated hydraulic conductivity	SATHC	m/h	0.01	0.60
	Soil porosity	PORO	-	0.2	0.8
	Soil pH	pH	-	4.5	9.1
	Initial soil organic carbon content	ISOC	kg C/kg	0	0.5
	Depth of top soil with uniform SOC content	SOCPU	m	0	0.30
	SOC decrease rate below top soil	SOCDA	-	0.5	5.0
	Initial soil nitrate nitrogen content	NO_3^--N	mg N/kg	8.5	15.5
	Initial soil ammonium nitrogen content	NH_4^+-N	mg N/kg	0.85	1.50
	Soil salinity index	SALI	-	0	100

2.4.2. Crop Model Input Parameters and Output Response Variables for Sensitivity Analysis

A crop model is a complex nonlinear dynamic system, and its output variables are functions of multiple input parameters. Inaccurate input parameter values may lead to unreasonable or even erroneous simulation results. During crop model parameter calibration, it is generally impractical to estimate all model parameters because of limitations in observation conditions and sample size. Therefore, it is necessary to identify a sensitive parameter set through sensitivity analysis before model calibration, so that model parameters can be calibrated in a targeted manner. Previous studies have shown that sensitivity analysis should be conducted when crop models are applied under different field management practices and at different locations [14]. Therefore, in this study, parameter sensitivity analysis was performed based on field experiments with different starter nitrogen application rates in the Tongliao region. The DNDC model input parameters used for sensitivity analysis included 12 maize crop parameters and 13 soil parameters (Table 3).

Based on experimental data from North America and China, the DNDC model has established a set of default crop parameter values for maize. These parameters are key inputs for simulating maize phenological dynamics and yield (Table 3). However, a single parameter set is unlikely to adequately represent maize parameters for both China and Europe/North America. Therefore, Li et al. [24] calibrated crop parameters suitable for maize production in China. In the present study, the upper and lower bounds of crop parameters were set to 130% and 70% of the calibrated Chinese maize parameters, respectively. It should be noted that the Chinese maize parameters determined by Li et al. [24] did not distinguish between summer maize and spring maize. Therefore, the upper bounds of the C/N ratios of grain, leaves, stems, and roots were extended to the calibrated values reported for spring maize [25]. The lower bound of water demand was set to 130 kg water/g DM, while the upper and lower bounds of stem, leaf, and grain fractions, as well as optimum temperature, were set to 130% and 70% of the mean values across spring maize cultivars, respectively [17]. In addition, Jiang et al. [26] set the N fixation index to 0, whereas Leng et al. [27] set the N fixation index to 1. Accordingly, the upper and lower bounds of the N fixation index in this study were set to 1 and 0, respectively. The ranges of the remaining crop and soil parameters were derived from the study of Qin et al. [28] and the recommended ranges of the DNDC model.

The DNDC crop model simulates spring maize growth at a daily time step and outputs time-varying variables, namely growth-process variables. Accurate simulation of these process variables is essential for reliably estimating final outputs such as yield. Therefore, analyzing the effects of parameters on both growth-process variables and final output variables is important for understanding and applying crop models. In this study, growth-process variables, including daily soil temperature, daily soil moisture, and daily cumulative N_2O emissions, together with the final output variable, yield, were selected as output responses for sensitivity analysis (Table 4).

Table 4. Output variables for global sensitivity analysis in the DNDC model.

Description	Unit
Soil temperature	°C
Soil moisture	cm^3/cm^3
Cumulative N_2O emissions	kg N/ha
Yield	kg C/ha

2.4.3. Sensitivity Analysis of Model Parameters Based on the EFAST Method

To evaluate the sensitivity of model output variables to input parameters, both local and global sensitivity analysis methods are widely used. Local sensitivity analysis focuses on the effect of changes in a single parameter on model outputs and is generally suitable for linear models. In contrast, global sensitivity analysis quantifies the effects of individual parameters and their interactions on model outputs by allocating the uncertainty in output variables to all input parameters. Among global sensitivity analysis methods, the variance-based EFAST method has been widely applied. This method combines the ability of the FAST method to account for the effects of parameter interactions with the high sampling efficiency of Sobol's method. Therefore, in this study, the EFAST method was used to analyze the effects of input parameters (Table 3) on model outputs (Table 4). The EFAST method decomposes the total variance of the model output, $V(Y)$, according to the contribution of each input parameter to the model output variables [29,30]:

$$V(Y) = \sum_{i=1}^{n} V_i + \sum_{1 \leq i \leq j \leq n} V_{ij} + \cdots + V_{12\cdots n} \tag{6}$$

where V_i represents the variance in the model output caused by the independent variation of each parameter, and V_{ij} to $V_{12...n}$ represent the variance in the model output caused by interactions among the n parameters. In this study, the total-order sensitivity index (ST_i; Equation (7)) was used to quantify the effects of parameter interactions on model outputs:

$$ST_i = \frac{V(Y) - V_{-i}}{V(Y)} \tag{7}$$

where V_{-i} denotes the sum of variances excluding the variance caused by the ith parameter. ST_i ranges from 0 to 1, with higher values indicating a greater influence of model input parameters on model output variables. At present, there is no universally accepted threshold for defining parameter sensitivity. In this study, parameters with $ST_i > 0.1$ were considered sensitive [14]. The ST_i values were calculated using SimLab 2.2 software (https://ec.europa.eu/jrc/en/samo/simlab, accessed on 15 June 2026). The sensitivity analysis procedure was as follows: (1) Determination of parameter distributions and ranges: when the distributions of crop model parameters were uncertain, these parameters were assumed to follow a uniform distribution. The variation ranges of the crop and soil parameters are shown in Table 3. (2) Generation of parameter sets: when using the EFAST method, the number of samples should be at least 100 times the number of parameters [31]. Therefore, based on the assumption of uniform distributions, Monte Carlo sampling was performed within the range of each parameter. A total of 2500 parameter sets were generated for the 25 crop and soil parameters for sensitivity analysis. (3) Generation of output variables: the parameter sets were converted into the input format required by the DNDC model using Python 3.12.3, and the DNDC crop model was then run to simulate spring maize growth. Output variables corresponding to the 2500 input parameter sets were obtained, including daily soil temperature, daily soil moisture, daily N_2O emissions, and yield. (4) Sensitivity analysis: the output variables corresponding to each parameter set were extracted from the DNDC crop model output files and organized into the file format required by SimLab. SimLab was then run to calculate the ST_i.

2.5. Parameter Calibration and Validation of the DNDC Model

In this study, the observed soil temperature, soil moisture, cumulative N_2O emissions, and maize yield data from 2024 were used to calibrate the model parameters, and the observed dataset from 2025 was used to validate the calibrated model. Two parameter sets were calibrated separately. Parameter set A included the sensitive crop and soil parameters identified through EFAST sensitivity analysis, whereas parameter set B included only the crop parameters commonly used for conventional DNDC calibration. This comparison was conducted to evaluate the effectiveness of parameter selection based on sensitivity analysis.

In this study, the differential evolution algorithm [32] was used to calibrate parameter set A and parameter set B. Differential evolution is a population-based optimization algorithm. It iteratively performs three main operations—mutation, crossover, and selection—on individuals within the population, thereby gradually eliminating inferior solutions, retaining and enhancing superior solutions, and ultimately approaching the global optimum. The core principle of the differential evolution algorithm is to generate mutant individuals using differential information among individuals in the population, increase solution diversity through crossover, and then select superior individuals for the next generation according to the fitness function until the termination criterion is satisfied. In this study, the population size was set to 60, the crossover probability to 0.7, the scaling factor to 0.8, and the maximum number of iterations to 200 generations [33]. The fitness function was defined as follows:

$$F(x) = \frac{1}{12}\sum\left[\frac{\left|N_t^{\mathrm{sim}}(x) - N_t^{\mathrm{obs}}\right|}{N_t^{\mathrm{obs}}} + \frac{1}{25} \times \frac{\left|S_t^{\mathrm{sim}}(x) - S_t^{\mathrm{obs}}\right|}{S_t^{\mathrm{obs}}} + \frac{1}{5} \times \frac{\left|H_t^{\mathrm{sim}}(x) - H_t^{\mathrm{obs}}\right|}{H_t^{\mathrm{obs}}} + \frac{\left|Y_t^{\mathrm{sim}}(x) - Y_t^{\mathrm{obs}}\right|}{Y_t^{\mathrm{obs}}}\right] \tag{8}$$

where $N_t^{\mathrm{sim}}(x)$, $S_t^{\mathrm{sim}}(x)$, $H_t^{\mathrm{sim}}(x)$, $Y_t^{\mathrm{sim}}(x)$ are the simulated values of cumulative N_2O emissions, soil temperature, soil moisture, and yield under treatment t (t = 1, 2, 3), respectively. $N_t^{\mathrm{obs}}(x)$, $S_t^{\mathrm{obs}}(x)$, $H_t^{\mathrm{obs}}(x)$, $Y_t^{\mathrm{obs}}(x)$ are the corresponding observed values. In Equation (8), the outer coefficient $1/12$ represents averaging across 12 variable–treatment combinations, namely four output variables—cumulative N_2O emissions, soil temperature, soil moisture, and yield—under three nitrogen treatments (N15, N30, and N45). The coefficients $1/15$ and $1/5$ represent the number of observations for the corresponding variables within each treatment and were used to calculate their mean relative errors.

2.6. Scenario Settings

To systematically evaluate the effects of total nitrogen application rate and starter nitrogen rate on maize yield and cumulative N_2O emissions, and to determine an appropriate nitrogen application strategy, the calibrated DNDC model was used to simulate yield and cumulative N_2O emissions under different nitrogen management scenarios. Eight total nitrogen application rates were established: 100 kg/ha (B1), 150 kg/ha (B2), 200 kg/ha (B3), 250 kg/ha (B4), 300 kg/ha (B5), 350 kg/ha (B6), 400 kg/ha (B7), and 450 kg/ha (B8). In addition, eight starter nitrogen proportions were set, corresponding to 0% (A1), 15% (A2), 25% (A3), 30% (A4), 35% (A5), 40% (A6), 45% (A7), and 50% (A8) of the total nitrogen application rate. A full-factorial design was adopted, generating a total of 64 scenarios. For the simulation of these 64 scenarios, the meteorological data used to drive the DNDC model were the mean values of the five-year period from 2021 to 2025. Soil properties during these five years were assumed to be consistent with those measured in the 2024 field experiment. Except for nitrogen application rate, all other field management practices were kept consistent with those used in local high-yielding fields. The values of crop and soil parameters were determined based on the results of the sensitivity analysis.

2.7. Statistical Indicators

In this study, the root mean square error (*RMSE*), normalized root mean square error (*nRMSE*), and average relative error (*ARE*) were used to evaluate the simulation performance of the DNDC model. These indicators were calculated as follows:

$$RMSE = \sqrt{\frac{1}{n}\sum_{i=1}^{n}(O_i - S_i)^2} \tag{9}$$

$$nRMSE = \frac{RMSE}{\overline{O}} \times 100\% \tag{10}$$

$$ARE = \frac{1}{n}\sum\left|\frac{O_i - S_i}{O_i}\right| \times 100\% \tag{11}$$

where O_i and S_i denote the observed and simulated values for the *i*th sample, respectively; $\overline{O}$ is the mean of the observed values; and n is the number of samples. *RMSE* quantifies the absolute difference between simulated and observed values and therefore reflects the overall magnitude of model error. *nRMSE* normalizes *RMSE* by the mean observed value, allowing the simulation errors of different variables to be compared on a relative scale. *ARE* quantifies the mean percentage deviation of simulated values from observed values across all samples. For all three indicators, lower values indicate better agreement between simulations and observations and, consequently, better model performance.

3. Results

3.1. Results of Parameter Sensitivity Analysis

3.1.1. Sensitivity of Daily Soil Temperature to Crop and Soil Parameters

As shown in Figure 4, the parameters with relatively strong effects on daily soil temperature were PORO, SOCPU, SOCDA, LCN, MYIELD, RCN, NFIX, SATHC, SCN, SF, ISOC, and NO_3^-–N, all of which had sensitivity index values greater than 0.1. Among them, the global sensitivity indices of PORO, SOCPU, SOCDA, and LCN were all greater than 0.5, indicating that these parameters exerted substantial influences on daily soil temperature throughout the entire growing season. The parameters with relatively weak effects included CLAY, WILP, BD, NH_4^+–N, THERD, GCN, SALI, FC, GF, WATD, pH, OPTTEM, and LF, whose global sensitivity indices were all lower than 0.1. In addition, the starter nitrogen application level had only a minor effect on the global sensitivity indices.

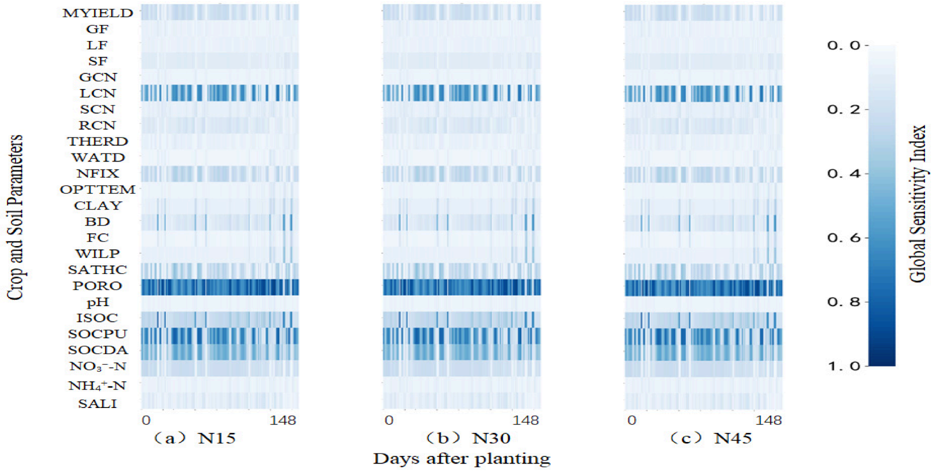

Figure 4. Sensitivity of daily soil temperature to crop and soil parameters under different starter nitrogen application rates. N15, N30, and N45 indicate that starter nitrogen accounted for 15%, 30%, and 45% of the total nitrogen application rate, respectively.

3.1.2. Sensitivity of Daily Soil Moisture to Crop and Soil Parameters

As shown in Figure 5, the parameters with relatively strong effects on daily soil moisture were WILP, FC, SOCDA, NO_3^-–N, RCN, and THERD. Among all parameters and treatments, WILP had the greatest influence on daily soil moisture, with a global sensitivity index of approximately 0.9, and its sensitivity was almost unaffected by changes in the starter nitrogen application rate. MYIELD, GF, LF, GCN, LCN, SCN, WATD, NFIX, OPTTEM, CLAY, BD, SATHC, PORO, pH, ISOC, SOCPU, NH_4^+–N, and SALI had relatively minor effects on daily soil moisture, with global sensitivity indices lower than 0.1. The starter nitrogen application level had little effect on the global sensitivity indices of the parameters, and the ranking of parameter sensitivity was generally consistent among treatments.

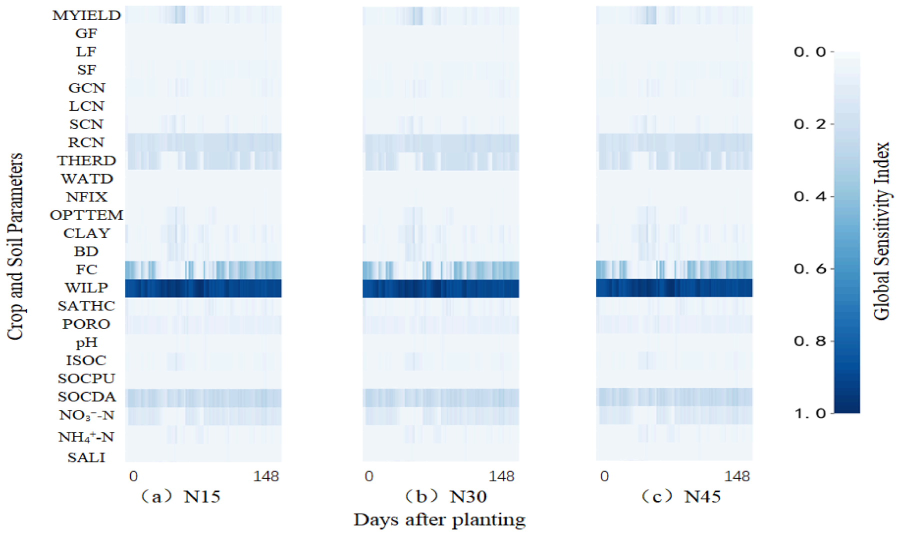

Figure 5. Sensitivity of daily soil moisture to crop and soil parameters under different starter nitrogen application rates. The meanings of N15, N30, and N45 are the same as those in Figure 4.

3.1.3. Sensitivity of Cumulative N_2O Emissions to Crop and Soil Parameters

As shown in Figure 6, the parameters that exerted relatively strong effects on cumulative N_2O emissions were GF, GCN, RCN, CLAY, BD, WILP, PORO, pH, ISOC, SOCPU, SOCDA, NO_3^-–N, and SALI, with global sensitivity indices greater than 0.1. Among these parameters, PORO showed the highest global sensitivity index, with a value of approximately 0.5; however, ISOC also exhibited a relatively high sensitivity index, indicating that both soil pore structure and initial soil organic carbon content were important factors controlling simulated cumulative N_2O emissions. The global sensitivity indices of MYIELD, SF, LF, LCN, SCN, THERD, WATD, NFIX, OPTTEM, FC, and SATHC were all lower than 0.1, indicating that these parameters had relatively minor effects on cumulative N_2O emissions. In addition, the starter nitrogen application rate had little influence on the global sensitivity indices of the parameters.

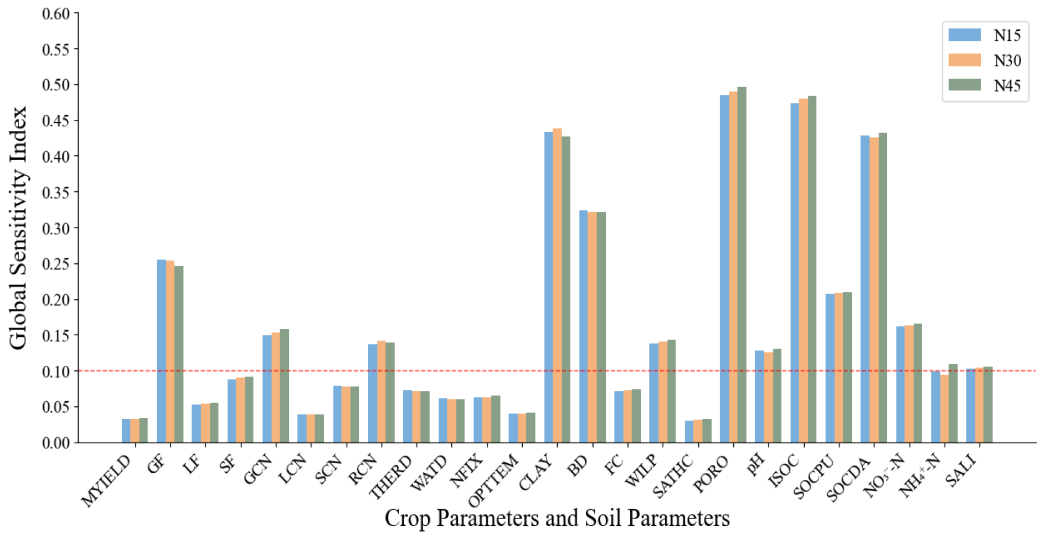

Figure 6. Sensitivity of cumulative N_2O emissions to crop and soil parameters under different starter nitrogen application rates. The meanings of N15, N30, and N45 are the same as those in Figure 4. The red dashed line indicates the threshold value of the global sensitivity index at 0.1.

3.1.4. Sensitivity of Yield to Crop and Soil Parameters

As shown in Figure 7, the parameters with relatively strong effects on yield were MYIELD, SF, CLAY, SOCDA, NH_4^+–N, GCN, SALI, THERD, LCN, BD, WATD, GF, FC, WILP, and RCN, all of which had global sensitivity indices greater than 0.1. Among them, MYIELD, SF, CLAY, SOCDA, and NH_4^+–N were the core parameters affecting yield simulation, with global sensitivity indices greater than 0.4. MYIELD had the highest sensitivity index, with a value of approximately 0.65. In contrast, LF, SCN, NFIX, OPTTEM, SATHC, PORO, pH, ISOC, SOCPU, and NO_3^-–N had relatively minor effects on yield, with global sensitivity indices lower than 0.1. As the starter nitrogen application rate increased, the effects of GF, RCN, THERD, CLAY, BD, WILP, SATHC, and ISOC on yield decreased. The global sensitivity indices of SF and GCN increased with increasing starter nitrogen application rate. The sensitivity indices of NH_4^+–N and SCN first increased and then decreased as the starter nitrogen application rate increased. In contrast, the global sensitivity indices of MYIELD, LF, LCN, WATD, NFIX, OPTTEM, FC, PORO, pH, SOCPU, SOCDA, NO_3^-–N, and SALI gradually decreased with increasing starter nitrogen application rate.

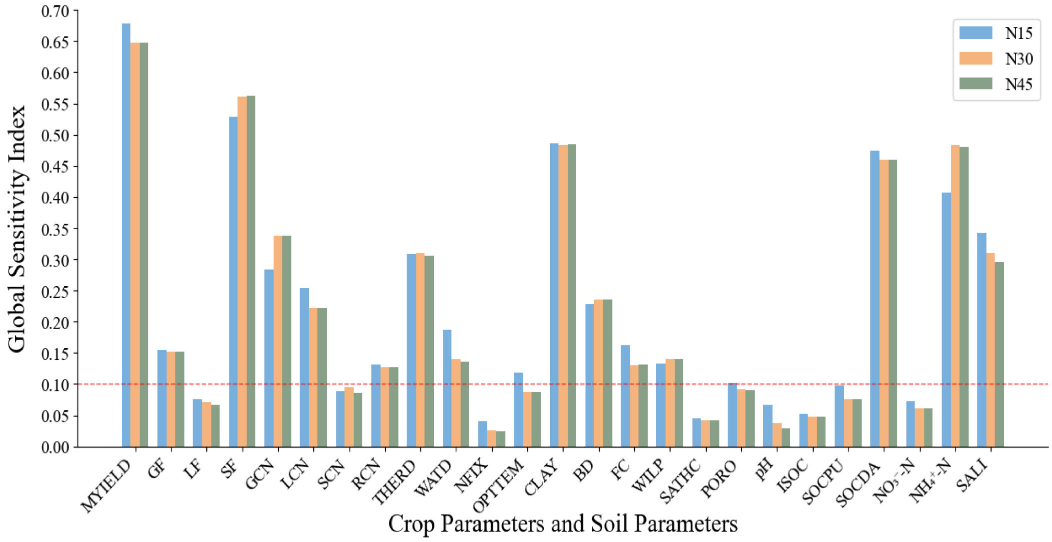

Figure 7. Sensitivity of yield to crop and soil parameters under different starter nitrogen application rates. The meanings of N15, N30, and N45 are the same as those in Figure 4. The red dashed line indicates the threshold value of the global sensitivity index at 0.1.

3.2. Calibration and Validation of Model Parameters

In this study, parameter set A and parameter set B were calibrated separately. Parameter set B consisted of 11 crop parameters commonly calibrated in previous DNDC studies, whereas parameter set A was determined based on EFAST sensitivity analysis. The ST_i of all crop and soil parameters were ranked for soil temperature, soil moisture, cumulative N_2O emissions, and yield. Parameters with $ST_i > 0.1$ were regarded as sensitive. To keep the number of calibrated parameters consistent between the two parameter sets, the top 11 sensitive parameters were selected to constitute parameter set A (Table 5).

Table 5. Calibrated parameter set A and conventional parameter set B.

Parameter Set A	Value	Parameter Set B	Value
MYIELD (kg C/ha)	4992	MYIELD (kg C/ha)	5150
LCN	37	LCN	39
SF	0.22	SF	0.19
GCN	37	GCN	38
THERD (°C)	3273	THERD (°C)	3110
GF	0.38	GF	0.40
SOCDA	2.4	LF	0.17
CLAY	0.42	SCN	57
PORO	0.5	OPTEM (°C)	27
WILP (cm^3/cm^3)	0.13	WATD (g/g)	165
SOCPU (m)	0.28	RCN	62

As shown in Table 5, compared with parameter set B, parameter set A retained only the commonly calibrated parameters MYIELD, LCN, SF, GCN, GF, and THERD, while additionally including the soil parameters SOCDA, CLAY, PORO, WILP, and SOCPU.

3.2.1. Model Parameter Calibration

Using parameter set A, the RMSE of simulated soil temperature under the N15 (Figure 8a), N30 (Figure 8b), and N45 (Figure 8c) treatments ranged from 1.24 to 1.30 °C, the nRMSE ranged from 5.05% to 5.44%, and the ARE ranged from 3.40% to 3.85%. In comparison, when parameter set B was used, the RMSE of simulated soil temperature across treatments ranged from 1.30 to 1.37 °C, the nRMSE ranged from 5.26% to

5.76%, and the ARE ranged from 3.65% to 4.08%. Compared with parameter set B, the simulated soil temperatures based on parameter set A were more closely distributed along the 1:1 line relative to the observed values, indicating higher simulation accuracy.

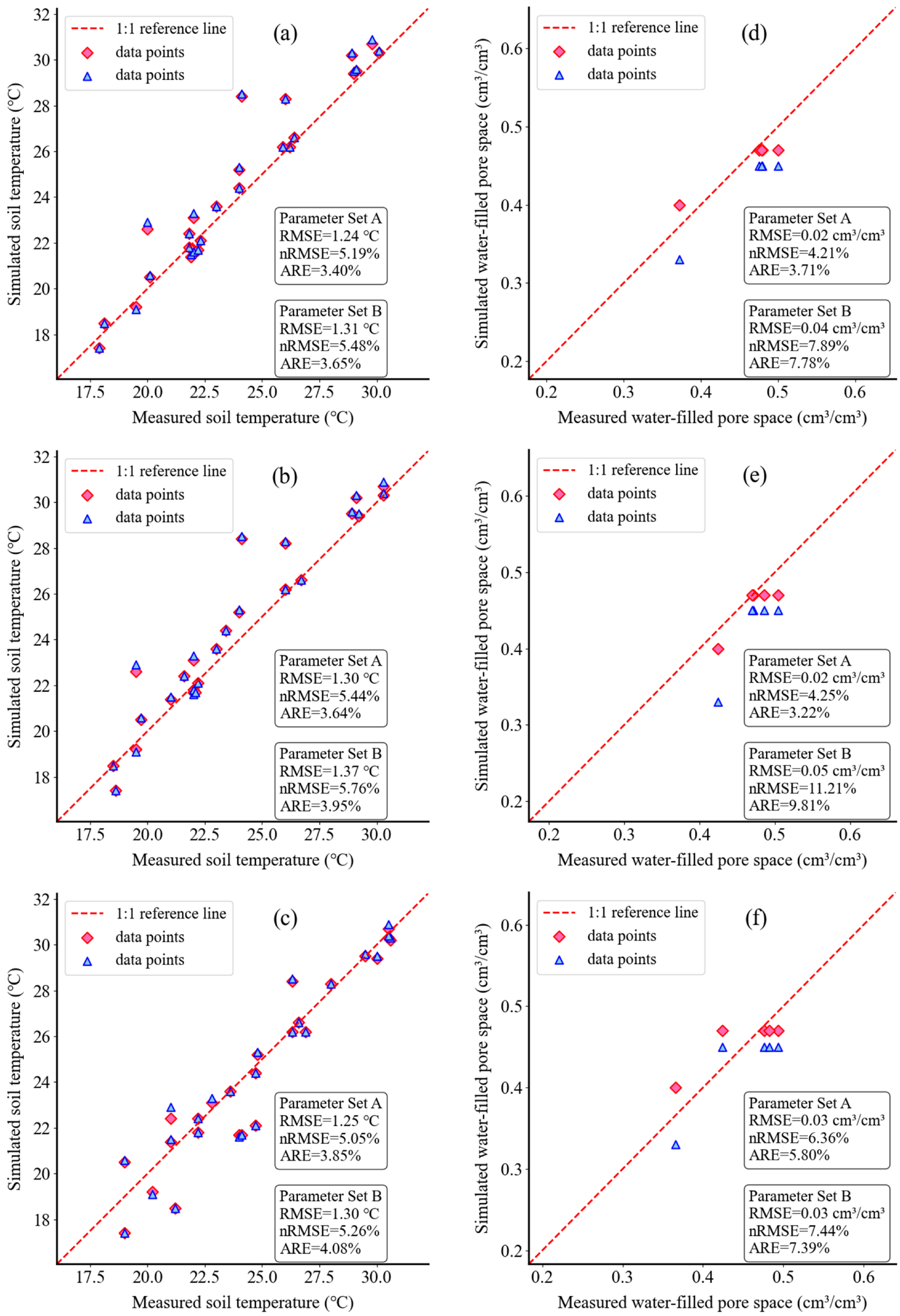

Figure 8. During the calibration stage, performance of the DNDC model in simulating 0–10 cm soil temperature (**a**–**c**) and 0–10 cm soil moisture (**d**–**f**) under the N15 (**a**,**d**), N30 (**b**,**e**), and N45 (**c**,**f**) treatments using parameter set A and parameter set B. Red diamonds and blue triangles represent the simulation results based on parameter set A and parameter set B, respectively.

As shown in Figure 8d, Figure 8e, and Figure 8f, when parameter set A was used, the RMSE, nRMSE, and ARE of simulated soil moisture ranged from 0.02 to 0.03 cm^3/cm^3, 4.21% to 6.36%, and 3.22% to 5.80%, respectively. When parameter set B was used, the RMSE, nRMSE, and ARE of simulated soil moisture ranged from 0.03 to 0.05 cm^3/cm^3, 7.44% to 11.21%, and 7.39% to 9.81%, respectively. Compared with parameter set B, parameter set A reduced the RMSE, nRMSE, and ARE by 0.02 cm^3/cm^3, 3.91%, and 4.09%, respectively, indicating that the model achieved higher accuracy in simulating soil moisture when parameter set A was used.

As shown in Figure 9a, the observed cumulative N_2O emissions differed significantly among treatments ($p < 0.05$), following the order N45 > N30 > N15. The RMSE, nRMSE, and ARE of cumulative N_2O emissions simulated by the DNDC model using parameter set A were 0.01 kg N/ha, 6.58%, and 4.56%, respectively, whereas those simulated using parameter set B were 0.01 kg N/ha, 12.09%, and 18.16%, respectively. These results indicate that parameter set A improved the simulation accuracy of cumulative N_2O emissions, as reflected by lower nRMSE and ARE values, which decreased by 5.51% and 13.60%, respectively. As shown in Figure 9b, the observed yield under N45 was significantly lower than those under N15 and N30, whereas no significant difference was observed between N15 and N30 ($p < 0.05$). The RMSE, nRMSE, and ARE of yield simulated by the DNDC model using parameter set A were all lower than those obtained using parameter set B. Compared with parameter set B, parameter set A reduced the RMSE, nRMSE, and ARE of yield simulation by 415.57 kg C/ha, 8.77%, and 10.17%, respectively.

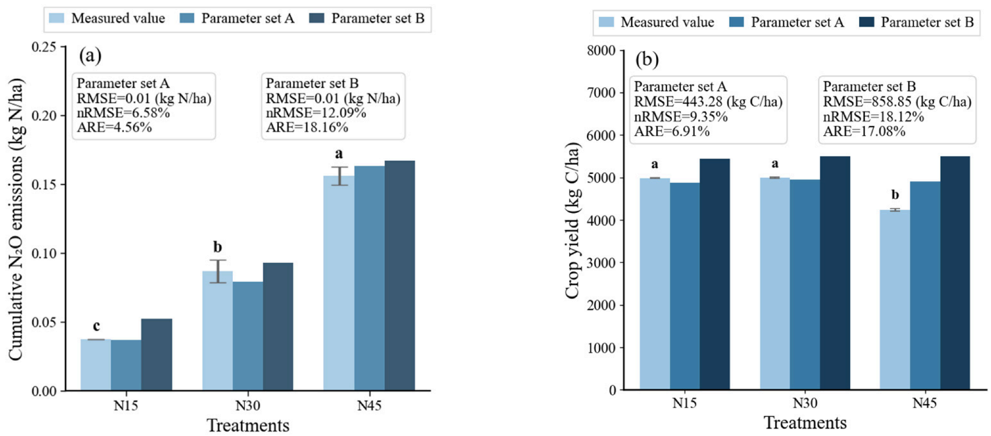

Figure 9. During the calibration stage, performance of the DNDC model in simulating (**a**) cumulative N_2O emissions and (**b**) yield using parameter set A and parameter set B. Different lowercase letters above the measured bars indicate significant differences among treatments at the 0.05 level; bars sharing the same letter are not significantly different.

3.2.2. Model Parameter Validation

As shown in Figure 10a–c, when parameter set A was used, the RMSE, nRMSE, and ARE of simulated soil temperature across treatments ranged from 0.96 to 1.14 °C, 3.83% to 4.53%, and 2.57% to 3.04%, respectively. When parameter set B was used, the corresponding RMSE, nRMSE, and ARE values ranged from 1.28 to 1.31 °C, 5.11% to 5.23%, and 4.35% to 4.53%, respectively. Both parameter sets achieved good performance in simulating soil temperature; however, parameter set A provided higher simulation accuracy. Compared with parameter set B, parameter set A reduced RMSE, nRMSE, and ARE by 0.27 °C, 1.08%, and 1.69%, respectively. The soil temperature values simulated by the DNDC model using parameter set A were more closely distributed around the 1:1 line relative to the observed values, indicating better model performance.

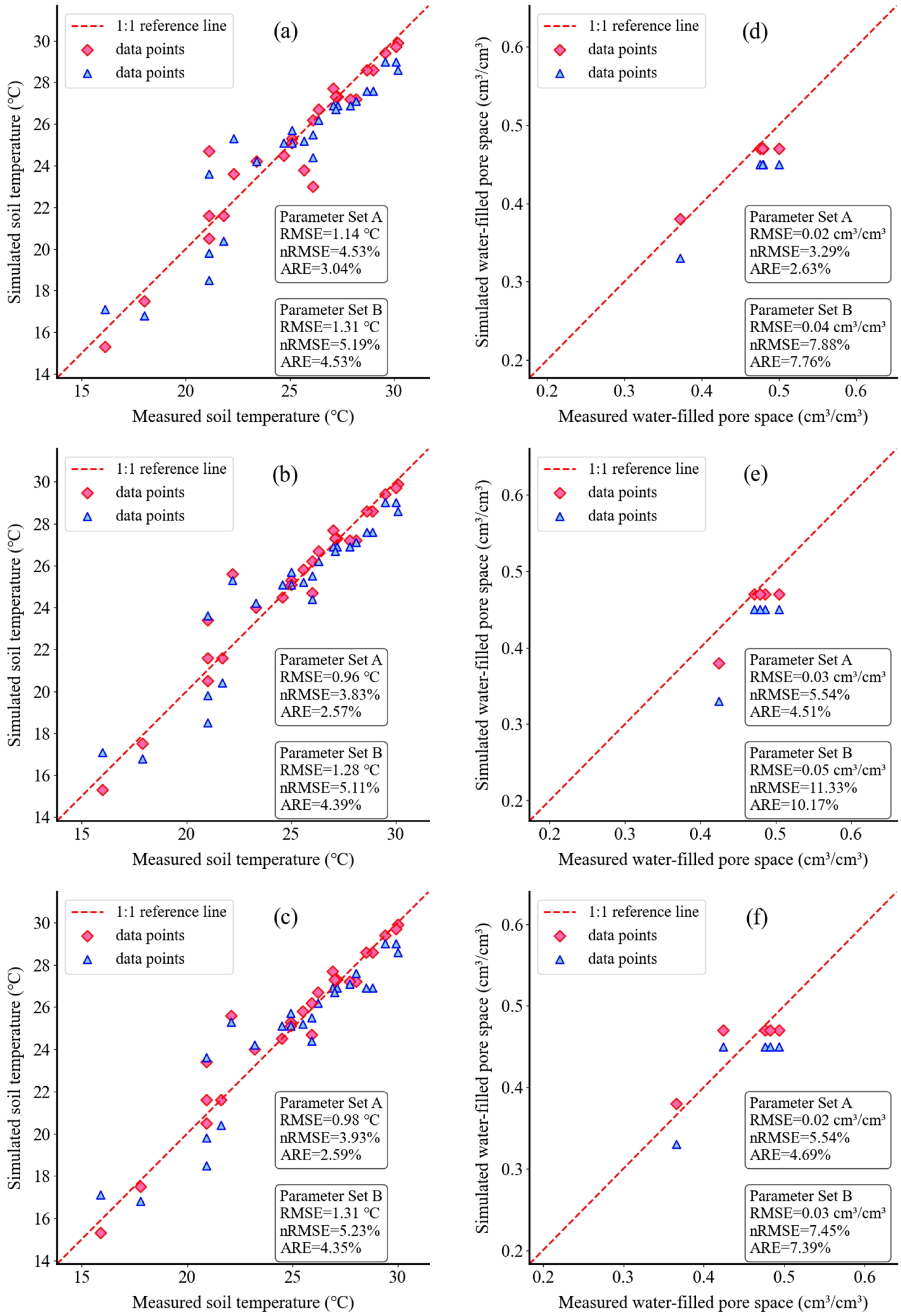

Figure 10. During the validation phase, performance of the DNDC model in simulating 0–10 cm soil temperature (**a**–**c**) and soil moisture (**d**–**f**) under the N15 (**a**,**d**), N30 (**b**,**e**), and N45 (**c**,**f**) treatments using parameter set A and parameter set B. Red diamonds and blue triangles represent the simulation results based on parameter set A and parameter set B, respectively.

As shown in Figure 10d–f, when parameter set A was used, the RMSE, nRMSE, and ARE of simulated soil moisture ranged from 0.02 to 0.03 cm^3/cm^3, 3.29% to 5.54%, and 2.63% to 4.69%, respectively. When parameter set B was used, the corresponding RMSE, nRMSE, and ARE values ranged from 0.03 to 0.05 cm^3/cm^3, 7.45% to 11.33%, and 7.39% to 10.17%, respectively. Compared with parameter set B, parameter set A reduced the RMSE, nRMSE, and ARE by 0.02 cm^3/cm^3, 4.10%, and 4.50%, respectively, indicating that the DNDC model achieved higher accuracy in simulating soil moisture when parameter set A was used.

As shown in Figure 11a, the observed cumulative N_2O emissions differed significantly among treatments ($p < 0.05$), following the order N45 > N30 > N15. The cumulative N_2O emissions simulated by the DNDC model using parameter set A were closer to the observed values across the three treatments. The RMSE, nRMSE, and ARE of cumulative N_2O emissions simulated using parameter set A were 0.01 kg N/ha, 14.98%, and 16.31%, respectively. In comparison, the corresponding values obtained using parameter set B were 0.03 kg N/ha, 30.16%, and 24.21%, respectively. Thus, parameter set A reduced the RMSE, nRMSE, and ARE by 0.02 kg N/ha, 15.18%, and 7.90%, respectively. As shown in Figure 11b, the observed yield under N45 was significantly lower than those under N15 and N30, whereas no significant difference was observed between N15 and N30 ($p < 0.05$). The DNDC model also achieved higher accuracy in simulating yield when parameter set A was used. The RMSE, nRMSE, and ARE were 163.92 kg C/ha, 3.27%, and 3.05%, respectively, which were 329.11 kg C/ha, 6.56%, and 6.45% lower than those obtained using parameter set B, respectively.

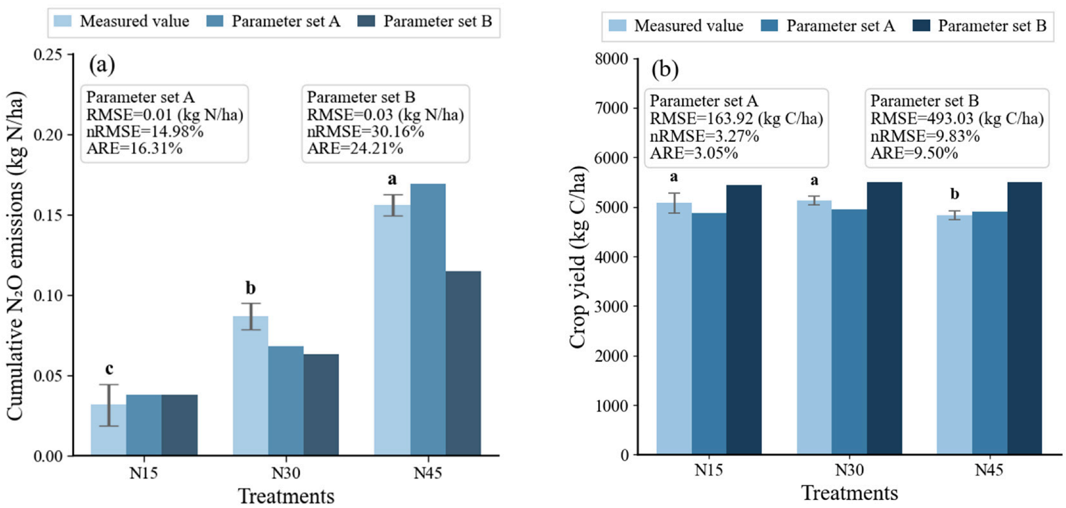

Figure 11. During the validation phase, performance of the DNDC model in simulating (**a**) cumulative N_2O emissions and (**b**) yield using parameter set A and parameter set B. Different lowercase letters above the measured bars indicate significant differences among treatments at the 0.05 level; bars sharing the same letter are not significantly different.

3.3. Scenario Simulation

3.3.1. Effects of Total Nitrogen Application Rate on Cumulative N_2O Emissions and Yield

Figure 12a shows the variation in cumulative N_2O emissions under the eight total nitrogen application scenarios. Cumulative N_2O emissions increased progressively with increasing total nitrogen application rate. The lowest cumulative N_2O emission was observed under the B1 scenario, at 0.32 kg N/ha, whereas the highest value occurred under the B8 scenario, reaching 3.55 kg N/ha. Figure 12b shows the effects of the eight total nitrogen application rates on spring maize yield. With increasing total nitrogen application rate, maize yield initially increased and then remained nearly unchanged. From B1 to B6, spring maize yield continuously increased, with the maximum yield reaching approximately 5000 kg C/ha. From B6 to B8, yield showed little further change.

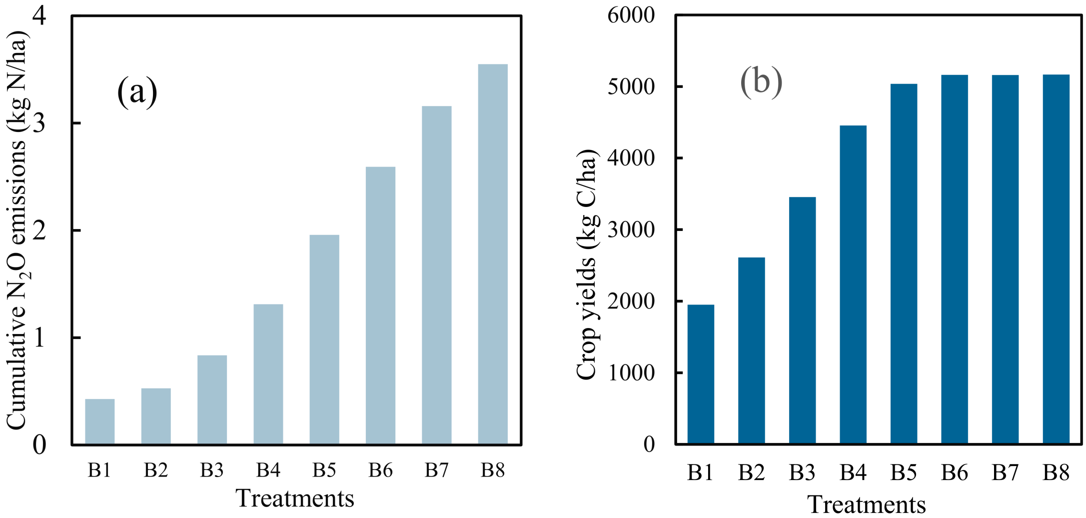

Figure 12. Effects of different total nitrogen application rate scenarios on (**a**) cumulative N_2O emissions and (**b**) grain yield in maize fields. B1–B8 indicate total nitrogen application rates of 100, 150, 200, 250, 300, 350, 400, and 450 kg/ha, respectively.

3.3.2. Effects of Starter Nitrogen Proportion on Cumulative N_2O Emissions and Yield

The analysis of variance showed that different starter nitrogen rates had significant effects on both spring maize yield and cumulative N_2O emissions ($p < 0.05$). Figure 13a shows the variation in cumulative N_2O emissions from maize fields under the eight starter nitrogen scenarios. Overall, cumulative N_2O emissions first decreased and then increased. The lowest value occurred under the A2 scenario, with an average cumulative N_2O emission of approximately 0.97 kg N/ha. From A3 to A8, cumulative N_2O emissions increased markedly, with the highest emission observed under the A8 scenario, reaching approximately 2.8 kg N/ha. The A1, A2, and A3 scenarios showed relatively low cumulative N_2O emissions, all below 1.3 kg N/ha. Figure 13b shows the variation in maize grain yield under the eight starter nitrogen scenarios. The highest maize yield was observed under the A1 scenario, at approximately 4861.4 kg C/ha, which was substantially higher than the yields under the other starter nitrogen levels. From A2 to A8, yield varied only slightly and remained clearly lower than that under the A1 scenario.

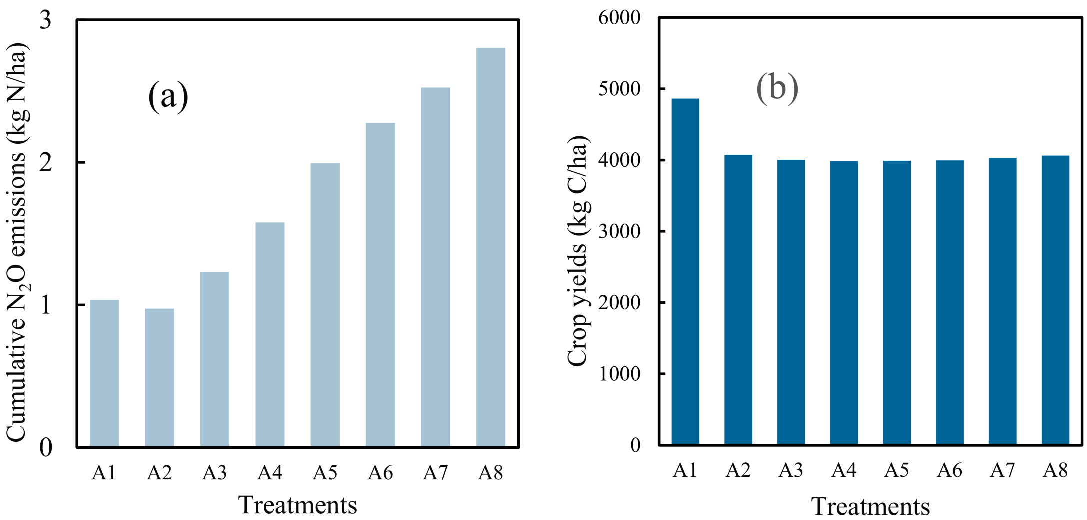

Figure 13. Effects of different starter nitrogen application scenarios on (**a**) cumulative N_2O emissions and (**b**) grain yield in maize fields. A1–A8 indicate starter nitrogen proportions of 0%, 15%, 25%, 30%, 35%, 40%, 45%, and 50% of the total nitrogen application rate, respectively.

3.3.3. Interactive Effects of the Proportion of Total Nitrogen Applied as Starter Fertilizer and Total Nitrogen Application Rate on Cumulative N_2O Emissions

The interactive effects of starter nitrogen proportion and total nitrogen application rate on cumulative N_2O emissions from maize fields were further investigated (Figure 14). Overall, cumulative N_2O emissions increased with increasing total nitrogen application rate, as indicated by the gradual color transition from blue to orange-red, suggesting that higher total nitrogen inputs substantially increased the risk of soil N_2O emissions. At low total nitrogen application rates, differences in cumulative N_2O emissions among starter nitrogen proportions were relatively small. For example, under the B1 scenario, cumulative N_2O emissions across different starter nitrogen proportion levels ranged only from 0.4154 to 0.4329 kg N/ha. As the total nitrogen application rate increased, the emission-enhancing effect of increasing starter nitrogen proportion became more pronounced. This pattern was particularly evident under the B6–B8 scenarios, where a higher proportion of nitrogen applied as starter fertilizer resulted in greater cumulative N_2O emissions.

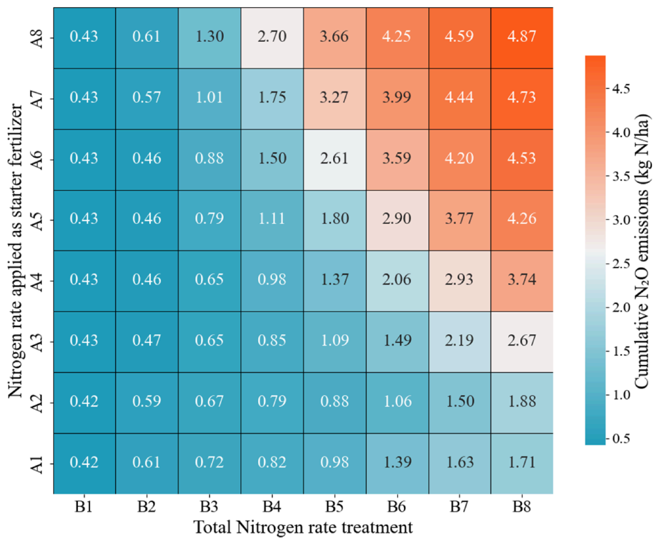

Figure 14. Interactive effects of starter nitrogen proportion and total nitrogen application rate on cumulative N_2O emissions.

The lowest cumulative N_2O emission was observed under the A1B1 treatment, at 0.4154 kg N/ha, whereas the highest value occurred under the A8B8 treatment, reaching 4.8714 kg N/ha, approximately 11.7 times higher than the lowest value. Under the highest total nitrogen application level, B8, cumulative N_2O emissions increased from 1.7122 to 4.8714 kg N/ha as the starter nitrogen level increased from A1 to A8. This indicates that, under high total nitrogen input conditions, increasing the starter nitrogen proportion further intensified N_2O emissions. In contrast, under relatively low total nitrogen application rates, the effect of starter nitrogen allocation on N_2O emissions was comparatively limited.

3.3.4. Interactive Effects of the Proportion of Total Nitrogen Applied as Starter Fertilizer and Total Nitrogen Application Rate on Maize Yield

The interactive effects of starter nitrogen proportion and total nitrogen application rate on maize yield were further analyzed (Figure 15). Overall, maize yield increased with increasing total nitrogen application rate, but yield responses differed among starter nitrogen proportion levels. Under low total nitrogen application rates (B1–B3), treatments with lower starter nitrogen proportions produced higher yields. In the A1 treatment, yield increased from 2464 kg C/ha under B1 to 3976 kg C/ha under B3, and these values were higher than those observed under treatments with higher starter nitrogen proportions. At the same low nitrogen level, yield generally decreased as the starter nitrogen proportion increased. For example, under B1, yield decreased from 2464 kg C/ha in A1 to 1597 kg C/ha in A8, indicating that allocating a larger proportion of total nitrogen as starter fertilizer was unfavorable for yield formation under low total nitrogen input. As the total nitrogen application rate increased to moderate levels (B4–B5), yield increased markedly across treatments. Under B5, most treatments approached or reached 5000 kg C/ha, with the highest yield observed in A1B5, reaching 5519 kg C/ha. When the total nitrogen application rate further increased to B6–B8, yield under treatments with higher starter nitrogen proportions remained relatively stable at approximately 5000 kg C/ha showing a clear plateau effect. In contrast, the treatment without starter nitrogen application, A1, maintained relatively high yield levels, reaching 6322, 6347, and 6347 kg C/ha under B6, B7, and B8, respectively.

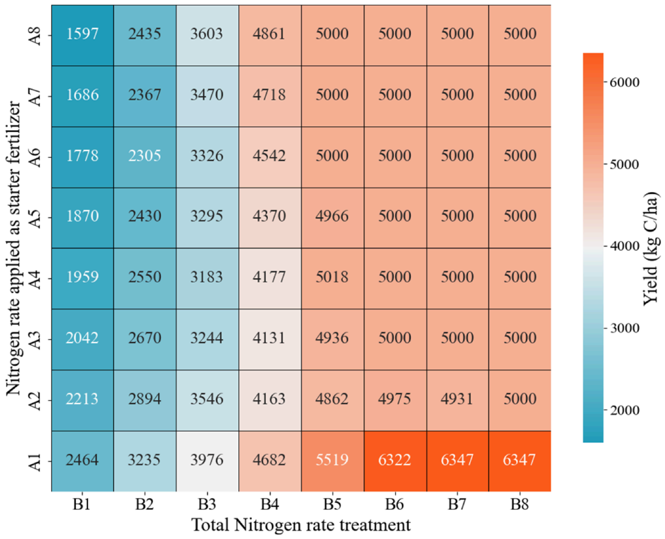

Figure 15. Interactive effects of starter nitrogen proportion and total nitrogen application rate on crop yield.

Overall, the B5A1 scenario, corresponding to a total nitrogen application rate of 300 kg/ha with no nitrogen applied as starter fertilizer, achieved relatively high yield while maintaining low cumulative N_2O emissions. Therefore, this scenario can be recommended as an appropriate nitrogen application strategy for maize production in the Tongliao region.

4. Discussion

4.1. Sensitivity Analysis

In this study, a global sensitivity analysis method was used to systematically evaluate the effects of crop and soil parameters in the DNDC model on the simulation of soil temperature, soil moisture, cumulative N_2O emissions, and maize yield under different starter nitrogen application proportions in the Tongliao region.

Soil temperature simulation was mainly affected by parameters such as PORO, SOCPU, and SOCDA, among which PORO had the highest global sensitivity index. This indicates that soil pore structure is a key factor influencing the simulation of soil thermal processes in the DNDC model [34]. Soil porosity affects soil heat capacity, thermal conductivity, and coupled water–heat transport processes by altering the relative proportions of solid phase, water, and air in the soil. Therefore, changes in soil porosity can modify the model-simulated dynamics of soil temperature [35]. SOCPU and SOCDA also showed high sensitivity to soil temperature, suggesting that the distribution of soil organic carbon within the soil profile can influence the soil thermal environment [36]. On the one hand, organic matter content and its distribution can alter soil aggregate structure, bulk density, and pore composition [36]. On the other hand, their effects on soil water-holding capacity and water redistribution can indirectly regulate heat conduction processes [36]. Therefore, in this spring maize system, calibrating only crop growth parameters may be insufficient to adequately represent variations in soil temperature. Soil porosity and soil organic carbon profile parameters should therefore be considered important targets for localized model calibration.

Soil moisture was most sensitive to WILP and FC, particularly WILP, which showed consistently high sensitivity indices across all treatments. WILP and FC represent the lower limit of soil water availability and field water-holding capacity, respectively, and are key hydraulic parameters used by the DNDC model to calculate soil water balance and crop-available water [35]. The high sensitivity of WILP indicates that, under the soil conditions and shallow-buried drip irrigation system of the study area, the lower threshold of soil water availability strongly affected the model's estimation of soil moisture dynamics [37]. The relatively high sensitivity of FC suggests that soil water-storage capacity determines the extent to which irrigation and precipitation inputs are retained in the root zone, thereby affecting WFPS, crop water stress, and subsequent nitrogen transformation processes [38]. Therefore, accurate measurement or calibration of soil hydraulic parameters is fundamental for improving the DNDC model's ability to simulate soil moisture in irrigated maize fields.

Cumulative N_2O emissions showed high sensitivity to PORO, ISOC, CLAY, BD, SOCDA, SOCPU, NO_3^-–N, and several crop carbon–nitrogen allocation parameters, indicating that N_2O emission processes are jointly regulated by soil aeration status, carbon and nitrogen substrate availability, and crop nitrogen uptake [39]. PORO and ISOC were both important sensitive parameters for simulating N_2O emissions. PORO showed the highest sensitivity, suggesting that soil pore structure affects nitrification–denitrification processes by regulating soil moisture, gas diffusion, and oxygen supply [34]. Meanwhile, the high sensitivity of ISOC indicates that initial soil organic carbon content strongly affects N_2O production by regulating carbon substrate availability for microbial activity and denitrification [40]. In general, well-aerated conditions favor nitrification, whereas higher WFPS and restricted gas diffusion are more conducive to denitrification and N_2O production [41]. The sensitivity of CLAY and BD further indicates that soil texture and compaction alter the soil microbial environment by affecting pore connectivity, water retention capacity, and gas transport rates, thereby influencing the intensity of N_2O emissions [34]. The high sensitivity of ISOC, SOCPU, and SOCDA suggests that soil organic carbon content and its vertical distribution are important factors controlling N_2O emissions [42]. This is because organic carbon can serve as an electron donor for denitrifying microorganisms and can also affect mineral nitrogen availability by regulating microbial activity and nitrogen mineralization processes [43]. Meanwhile, crop parameters such as GF, GCN, and RCN also showed certain sensitivity to N_2O emissions, indicating that crop biomass allocation and plant nitrogen demand can indirectly regulate N_2O emissions by influencing crop nitrogen uptake capacity and residual soil mineral nitrogen. Therefore, the simulation of N_2O emissions is not determined solely by nitrogen application rate, but rather by the combined effects of soil physical structure, carbon and nitrogen substrate supply, and crop nitrogen uptake.

Yield was most sensitive to parameters such as MYIELD, SF, CLAY, SOCDA, and NH_4^+–N. Among them, MYIELD directly represents the potential productivity of the cultivar, and its high sensitivity is consistent with the structural characteristics of the crop growth module in the DNDC model. Biomass allocation parameters, such as SF and GF, affect the partitioning of assimilates among stems, leaves, and grains, thereby determining final grain yield [44]. Notably, soil parameters, including CLAY, SOCDA, BD, FC, and WILP, also showed relatively high sensitivity to yield, indicating that soil water-holding capacity, root-zone aeration, organic carbon distribution, and initial nitrogen supply jointly influence yield formation in spring maize [45]. The high sensitivity of NH_4^+–N suggests that initial mineral nitrogen availability plays an important role in model-based yield simulation. This may be particularly relevant under varying starter nitrogen proportions, where the coordination between nitrogen supply during the seedling stage and nitrogen uptake from subsequent topdressing may alter the model response to yield formation processes.

Therefore, in the localized application of the DNDC model, crop growth parameters should be incorporated together with soil hydraulic parameters, pore structure parameters, and soil organic carbon distribution parameters into the calibration parameter set. This approach can reduce parameter uncertainty and improve the applicability of the model under different nitrogen management scenarios.

4.2. Analysis of DNDC Model Simulation Accuracy

In this study, both parameter set A, selected based on sensitivity analysis, and the conventional crop parameter set B were calibrated. The results showed that, compared with parameter set B, parameter set A provided better simulations of soil temperature, soil moisture, cumulative N_2O emissions, and yield in shallow-buried drip-irrigated spring maize fields in the Tongliao region.

For soil temperature simulation, both parameter sets showed good fitting performance, but the simulated values obtained using parameter set A were closer to the observed values. Compared with parameter set B, parameter set A reduced the RMSE, nRMSE, and ARE by 0.27 °C, 1.08%, and 1.69%, respectively (Figure 10). This result indicates that optimization of soil parameters can also improve the model simulation of soil thermal processes. After soil parameters such as PORO, SOCPU, and SOCDA were incorporated into parameter set A, the model was better able to represent soil heat transfer and coupled soil water–heat processes in the study area [46], thereby improving the accuracy of soil temperature simulation. For soil moisture simulation, parameter set A reduced the RMSE, nRMSE, and ARE by 0.02 cm^3/cm^3, 4.10%, and 4.50%, respectively, compared with parameter set B. Soil moisture dynamics are generally regulated by irrigation input, evapotranspiration, infiltration, and root water uptake across different irrigation systems. In the present shallow-buried drip irrigation system, the localized wetting pattern and repeated irrigation events may further increase the temporal variability of root-zone soil moisture. The inclusion of soil hydraulic parameters such as WILP, CLAY, and PORO in parameter set A improved the model response to changes in root-zone soil moisture, thereby enhancing the simulation performance for soil moisture [47].

The simulation results for cumulative N_2O emissions further demonstrate the important role of soil process parameters in DNDC-based greenhouse gas emission simulation. During the validation period, parameter set A reduced the RMSE, nRMSE, and ARE by 0.02 kg N/ha, 15.18%, and 7.90%, respectively, compared with parameter set B (Figure 11a). These results indicate that calibration based only on conventional crop parameters is insufficient to fully capture the complexity of N_2O production and emission processes. By simultaneously accounting for key factors such as soil structure, soil water status, and soil organic carbon distribution, parameter set A more accurately represented the response of soil nitrogen transformation processes to nitrogen management [34]. For yield simulation, parameter set A also outperformed parameter set B. During the validation period, the RMSE, nRMSE, and ARE of yield simulated using parameter set A were reduced by 329.11 kg C/ha, 6.56%, and 6.45%, respectively, compared with parameter set B (Figure 11b). This suggests that yield formation is controlled not only by crop parameters such as MYIELD, GF, SF, and THERD, but also by soil water supply, the root-zone environment, and nitrogen availability [48]. By incorporating sensitive soil parameters, parameter set A improved the model representation of the crop growth environment and therefore showed greater stability in yield simulation.

4.3. Analysis of Scenario Simulation Results

Based on the calibrated DNDC model, 64 nitrogen management scenarios were constructed by combining different total nitrogen application rates and starter nitrogen proportions to analyze their effects on spring maize yield and cumulative N_2O emissions. Regarding starter nitrogen proportion, the lowest cumulative N_2O emissions occurred under the A2 scenario, whereas the highest emissions were observed under the A8 scenario. In contrast, yield was highest under the A1 scenario, while yields under A2–A8 were markedly lower and showed only minor differences among these scenarios. These results indicate that, under shallow-buried drip irrigation and split topdressing conditions, increasing the proportion of nitrogen applied as starter fertilizer did not substantially promote yield formation, but instead may have increased nitrogen accumulation in the root zone during the seedling stage, thereby enhancing the risk of subsequent N_2O emissions. During the seedling stage, spring maize has limited nitrogen uptake capacity. Concentrating excessive nitrogen fertilizer at sowing can easily lead to asynchrony between nitrogen supply and crop demand [49]. Therefore, appropriately reducing the starter nitrogen proportion and shifting nitrogen supply to the rapid growth stages of maize may help improve nitrogen use efficiency and reduce nitrogen losses [49]. Regarding total nitrogen application rate, N_2O emissions were relatively low under low nitrogen input, but yield was limited by insufficient nitrogen supply. Under moderate nitrogen input, yield increased markedly. Under high nitrogen input, however, the yield increase diminished and gradually reached a plateau, whereas N_2O emissions continued to increase. Previous studies have also shown that N_2O emissions often exhibit a nonlinear response to nitrogen fertilizer input, and excessive nitrogen application can substantially amplify emission risks without a corresponding increase in yield [45].

The interaction between total nitrogen application rate and starter nitrogen proportion markedly affected N_2O emissions. At low total nitrogen application rates, differences in N_2O emissions among treatments with different starter nitrogen proportions were relatively small. As the total nitrogen application rate increased, the emission-enhancing effect of a high starter nitrogen proportion became increasingly pronounced. The lowest N_2O emission was observed under A1B1, whereas the highest emission occurred under A8B8, with the latter being approximately 11.7 times higher than the former. This indicates that the combination of high total nitrogen input and a high starter nitrogen proportion can substantially increase the risk of soil nitrogen surplus and N_2O emissions. The interaction between total nitrogen application rate and starter nitrogen proportion also markedly affected yield. Under low nitrogen application levels, B1–B3, a higher starter nitrogen proportion reduced yield. For example, under B1, yield decreased from 2464 kg C/ha in A1 to 1597 kg C/ha in A8, indicating that when total nitrogen input is limited, allocating an excessive proportion of nitrogen to the early growth stage may weaken nitrogen supply during the middle and late growth stages, thereby adversely affecting yield formation [50]. As the total nitrogen application rate increased to B4–B5, yield under different treatments increased substantially and gradually approached a high level, with relatively high yield observed under A1B5. Further increases in nitrogen input resulted in limited additional yield gains but increased N_2O emissions, suggesting that reducing the starter nitrogen proportion and strengthening topdressing during the middle and late growth stages are more conducive to synchronizing nitrogen supply with the peak nitrogen demand of maize [51].

Overall, A1B5, corresponding to a total nitrogen application rate of 300 kg/ha with no nitrogen applied as starter fertilizer, was selected as the preferred trade-off strategy. Although further increasing total nitrogen input may produce higher yield under some scenarios, it requires additional nitrogen fertilizer and increases cumulative N_2O emissions. In contrast, A1B5 maintained a relatively high yield while keeping N_2O emissions at a comparatively low level, thereby providing a better balance between yield performance, nitrogen input, and emission mitigation. Therefore, A1B5 can be considered a preferred nitrogen management strategy for achieving high yield and low emissions in spring maize production in the study area. It should be noted that A1B5 does not imply that starter nitrogen should be completely eliminated under all production conditions. Rather, it emphasizes that, under shallow-buried drip irrigation and split topdressing conditions, reducing the proportion of nitrogen applied at sowing and strengthening precise nitrogen supply during the middle and late growth stages can enhance the synergy between yield formation and N_2O emission mitigation.

4.4. Limitation

Several limitations of this study should be acknowledged. First, a no-fertilizer control was not included in the field experiment because the main objective was to evaluate the effects of different starter nitrogen proportions under the same total nitrogen input and to provide field data for DNDC model calibration under local high-yield fertigation conditions. This represents a limitation of the field experimental design, and future studies should include a no-fertilizer control to further quantify the absolute crop response to fertilizer application.

Second, the DNDC model was calibrated and validated using two years of field experimental data, with one year used for calibration and the other for validation. Although the calibrated model showed good performance in this study, long-term field observations under different weather conditions are still needed to further confirm the robustness of the scenario simulation results and the stability of the recommended nitrogen management strategy.

Third, the field experiment included starter nitrogen proportions of 15%, 30%, and 45%, whereas the scenario simulation further explored 0% and 50% starter nitrogen proportions. Therefore, the A1 and A8 scenarios represent model extrapolations beyond the calibration data. Although using a calibrated process-based model to explore broader management scenarios is a common approach in DNDC-based studies, the uncertainty associated with these extrapolated scenarios is expected to be higher than that of scenarios within the observed treatment range. Future field experiments should include no-starter-nitrogen and higher-starter-nitrogen treatments to further validate the simulated responses.

5. Conclusions

This study integrated EFAST-based global sensitivity analysis, the differential evolution algorithm, and the DNDC model to evaluate parameter sensitivity, model calibration, and nitrogen management optimization for shallow-buried drip-irrigated spring maize in the Tongliao region. The main conclusions are as follows: (1) DNDC model outputs were jointly controlled by crop and soil parameters. Soil temperature, soil moisture, cumulative N_2O emissions, and yield were affected by different parameter groups, indicating that both crop and soil parameters should be considered in sensitivity analysis and localized calibration for spring maize systems in this region. (2) The sensitivity-screened parameter set A performed better than the conventional crop-parameter set B. By incorporating key crop parameters and sensitive soil parameters, parameter set A improved the simulation accuracy of soil temperature, soil moisture, cumulative N_2O emissions, and yield. Therefore, it can provide a localized parameter set for DNDC applications in shallow-buried drip-irrigated spring maize systems. (3) Total nitrogen application rate and starter nitrogen proportion jointly affected spring maize yield and N_2O emissions. Increasing total nitrogen input continuously increased N_2O emissions, whereas yield increased initially and then tended to plateau. A higher starter nitrogen proportion did not markedly improve yield but increased N_2O emission risk under high nitrogen input. Considering yield performance, nitrogen input, and emission mitigation together, A1B5, corresponding to 300 kg N ha^{-1} with no nitrogen applied as starter fertilizer, was identified as the preferred trade-off strategy for achieving high yield and low emissions in the irrigated area of the West Liaohe Plain.

Author Contributions: Conceptualization, Y.W. and F.W.; data curation, Y.W. and J.L.; methodology, Y.W. and L.H.; writing—original draft, Y.W.; writing—review and editing, Y.W. and F.W. All authors have read and agreed to the published version of the manuscript.

Funding: This study was supported by the Interdisciplinary Research Fund Project of Inner Mongolia Agricultural University (BR241401), the Natural Science Foundation of Inner Mongolia Autonomous Region (2025QN03050), the Science and Technology Plan Program of Inner Mongolia Autonomous Region (2025YFDZ0027), and the Research Start-up Project for High-level and Outstanding Doctoral Talents (NDYB2023-12).

Data Availability Statement: The original contributions presented in this study are included in the article. Further inquiries can be directed to the corresponding authors.

Conflicts of Interest: The authors declare no conflicts of interest.

References

1. Qian, H.; Yuan, Z.; Chen, N.; Zhu, X.; Huang, S.; Lu, C.; Liu, K.; Zhou, F.; Smith, P.; Tian, H.; et al. Legacy effects cause systematic underestimation of N_2O emission factors. *Nat. Commun.* **2025**, *16*, 2775. [CrossRef] [PubMed]
2. Ball, M.; Hernandez-Ramirez, G. Nitrous oxide emissions and yields from potato production systems as influenced by nitrogen fertilization and irrigation: A meta-analysis. *Agron. J.* **2025**, *117*, e21720. [CrossRef]
3. Wang, C.; Shen, Y.; Fang, X.; Xiao, S.; Liu, G.; Wang, L.; Gu, B.; Zhou, F.; Chen, D.; Tian, H.; et al. Reducing soil nitrogen losses from fertilizer use in global maize and wheat production. *Nat. Geosci.* **2024**, *17*, 1008–1015. [CrossRef]
4. Palmero, F.; Davidson, E.A.; Guan, K.; Eagle, A.J.; Birgé, H.E.; Prasad, P.V.V.; Hefley, T.J.; Schussler, J.R.; Ciampitti, I.A. Environmental and societal costs of maize production decrease by addressing the uncertainty in nitrogen rate recommendations. *Nat. Commun.* **2026**, *17*, 2375. [CrossRef] [PubMed]
5. Shen, D.; Wang, K.; Zhou, L.; Fang, L.; Wang, Z.; Fu, J.; Zhang, T.; Liang, Z.; Xie, R.; Ming, B. Increasing planting density and optimizing irrigation to improve maize yield and water-use efficiency in Northeast China. *Agronomy* **2024**, *14*, 400. [CrossRef]
6. Preza-Fontes, G.; Miller, H.; Camberato, J.; Roth, R.; Armstrong, S. Corn yield response to starter nitrogen rates following a cereal rye cover crop. *Crop Forage Turfgrass Manag.* **2022**, *8*, e20187. [CrossRef]
7. Nasielski, J.; Deen, B. Nitrogen applications made close to silking: Implications for yield formation in maize. *Field Crops Res.* **2019**, *243*, 107621. [CrossRef]
8. Zhao, Z.; Cao, L.; Sha, Z.; Deng, J.; Chu, C.; Zhou, D.; Wu, S.; Lv, W. Impacts of fertilization optimization on N loss from paddy fields: Observations and DNDC modeling case study in Shanghai, China. *Soil Tillage Res.* **2020**, *199*, 104587. [CrossRef]
9. Yin, S.; Zhang, X.; Lyu, J.; Zhi, Y.; Chen, F.; Wang, L.; Liu, C.; Zhou, S. Carbon sequestration and emissions mitigation in paddy fields based on the DNDC model: A review. *Artif. Intell. Agric.* **2020**, *4*, 140–149. [CrossRef]
10. Shen, N.; Tan, J.; Mu, Q.; Huang, L.; Xue, W.; Wang, Y.; Gee Ooi, M.C.; Latif, M.T.; Yan, G.; Fat Nicky, L.Y.; et al. Recommendations on benchmarks for the DeNitrification–DeComposition model application in China: Insights from literature analysis. *Environ. Model. Softw.* **2025**, *190*, 106485. [CrossRef]
11. Ma, Y.; Qiao, Y.; Tang, Y.; Wu, Y.; Miao, S. Estimation of N_2O and CH_4 emissions in field study and DNDC model under optimal nitrogen level in rice-wheat rotation system. *Sci. Total Environ.* **2025**, *974*, 179168. [CrossRef] [PubMed]
12. Huang, Q.; Katayanagi, N.; Komatsuzaki, M.; Fumoto, T. Field Validation of the DNDC-Rice Model for Crop Yield, Nitrous Oxide Emissions and Carbon Sequestration in a Soybean System with Rye Cover Crop Management. *Agriculture* **2025**, *15*, 1525. [CrossRef]

13. Li, S.; Zhang, W.; Li, Y.; Liu, C.; Zhu, B.; Kihara, J.; Bolo, P.; Yao, Z.; Wang, K.; Han, S. Greenhouse gas footprints of maize cultivation systems in different climate zones: Field data validation and application of CNMM–DNDC as a hydro-biogeochemical model. *Adv. Atmos. Sci.* **2025**, *42*, 2365–2393. [CrossRef]
14. Wang, Y.; Guo, F.; Shen, H.; Xing, X.; Ma, X. Global Sensitivity Analysis and Evaluation of the DSSAT Model for Summer Maize (*Zea mays* L.) Under Irrigation and Fertilizer Stress. *Int. J. Plant Prod.* **2021**, *15*, 523–539. [CrossRef]
15. Wang, C.; Harrison, M.T.; Brown, H.; Qiao, Y.; Yin, X.; Yang, R.; Zhang, Y.; Zhou, M.; Liu, K. Global sensitivity analyses prior to parameter calibration significantly improves prediction quality. *Comput. Electron. Agric.* **2025**, *238*, 110750. [CrossRef]
16. Cui, H.; Zhu, H.; Zhang, F.; Wang, X.; Hou, S.; Feng, W. Soil amendments reduce CH_4 and CO_2 but increase N_2O and NH_3 emissions in saline-alkali paddy fields. *Sci. Total Environ.* **2024**, *924*, 171673. [CrossRef] [PubMed]
17. Fan, D.; Song, D.; Jiang, R.; He, P.; Shi, Y.; Pan, Z.; Zou, G.; He, W. Modelling adaptation measures to improve maize production and reduce soil N2O emissions under climate change in Northeast China. *Atmos. Environ.* **2024**, *319*, 120241. [CrossRef]
18. *GB 50288-2018*; National Standard of the People's Republic of China: Design Standard for Irrigation and Drainage Engineering. China Planning Press: Beijing, China, 2018.
19. Macharia, J.M.; Ngetich, F.K.; Shisanya, C.A. Parameterization, calibration and validation of the DNDC model for carbon dioxide, nitrous oxide and maize crop performance estimation in East Africa. *Heliyon* **2021**, *7*, e06977. [CrossRef] [PubMed]
20. Wang, S.; Lu, J.; Sun, S.; Hu, R.; Li, J.; Pang, J.; Yang, Y. Greenhouse gas emission characteristics of farmland in the Guanzhong region under varied water-nitrogen management measures based on the DNDC model. *Agric. Syst.* **2026**, *233*, 104628. [CrossRef]
21. Cheng, K.; Pan, G.; Smith, P.; Luo, T.; Li, L.; Zheng, J.; Zhang, X.; Han, X.; Yan, M. Carbon footprint of China's crop production—An estimation using agro-statistics data over 1993–2007. *Agric. Ecosyst. Environ.* **2011**, *142*, 231–237. [CrossRef]
22. Scott, I.S.P.C.; Nouwakpo, K.; Bjorneberg, D.; Rogers, C.; Vitko, L. Establishing a standard protocol for soil texture analysis using the laser diffraction technique. *Soil Sci. Soc. Am. J.* **2024**, *88*, 1691–1708. [CrossRef]
23. Ma, N.; Kang, J.; Lyu, K.; Tan, X.; Liu, S. Effects of straw return and planting density on maize yield and soil physicochemical properties. *J. Agric. Sci.* **2024**, *45*, 38–43. [CrossRef]
24. Li, H.; Wang, L.; Li, J.; Gao, M.; Zhang, J.; Zhang, J.; Qiu, J.; Deng, J.; Li, C.; Frolking, S. The development of China-DNDC and review of its applications for sustaining Chinese agriculture. *Ecol. Model.* **2017**, *348*, 1–13. [CrossRef]
25. Li, H.; Wang, L.; Qiu, J.; Li, C.; Gao, M.; Gao, C. Calibration of DNDC model for nitrate leaching from an intensively cultivated region of Northern China. *Geoderma* **2014**, *223–225*, 108–118. [CrossRef]
26. Jiang, Q.; Madramootoo, C.A.; Qi, Z. Soil carbon and nitrous oxide dynamics in corn (*Zea mays* L.) production under different nitrogen, tillage and residue management practices. *Field Crops Res.* **2022**, *277*, 108421. [CrossRef]
27. Leng, X.; Li, X.; Chen, N.; Zhang, J.; Guo, Y.; Ding, Z. Evaluating the effects of biodegradable film mulching and topdressing nitrogen on nitrogen dynamic and utilization in the arid cornfield. *Agric. Water Manag.* **2021**, *258*, 107166. [CrossRef]
28. Qin, X.; Wang, H.; Li, Y.; Li, Y.; McConkey, B.; Lemke, R.; Li, C.; Brandt, K.; Gao, Q.; Wan, Y.; et al. A long-term sensitivity analysis of the denitrification and decomposition model. *Environ. Model. Softw.* **2013**, *43*, 26–36. [CrossRef]
29. Xu, X.; Shen, S.; Xiong, S.; Ma, X.; Fan, Z.; Han, H. Water Stress is a Key Factor Influencing the Parameter Sensitivity of the WOFOST Model in Different Agro-Meteorological Conditions. *Int. J. Plant Prod.* **2021**, *15*, 231–242. [CrossRef]
30. Wang, Z.; Shi, Y.; Hou, C.; Zhang, P. Sensitivity analysis of simulated *Lycium barbarum* L. yield in the WOFOST model under different climate conditions. *Ecol. Model.* **2024**, *488*, 110602. [CrossRef]
31. Jin, X.; Li, Z.; Nie, C.; Xu, X.; Feng, H.; Guo, W.; Wang, J. Parameter sensitivity analysis of the AquaCrop model based on extended fourier amplitude sensitivity under different agro-meteorological conditions and application. *Field Crops Res.* **2018**, *226*, 1–15. [CrossRef]
32. Brest, J.; Sepesy Maučec, M. Comparative Study of Modern Differential Evolution Algorithms: Perspectives on Mechanisms and Performance. *Mathematics* **2025**, *13*, 1556. [CrossRef]
33. Das, S.; Suganthan, P.N. Differential Evolution: A Survey of the State-of-the-Art. *IEEE Trans. Evol. Comput.* **2011**, *15*, 4–31. [CrossRef]
34. Maillet, E.; Grossel, A.; Cousin, I.; Arbaret, L.; Cottenot, L.; Lacoste, M. What is the most relevant soil structure parameter to describe field-measured N_2O emissions? *Geoderma* **2025**, *453*, 117155. [CrossRef]
35. Li, C.; Frolking, S.; Frolking, T.A. A model of nitrous oxide evolution from soil driven by rainfall events: 1. Model structure and sensitivity. *J. Geophys. Res. Atmos.* **1992**, *97*, 9759–9776. [CrossRef]
36. He, Y.; He, W.; Wang, L.; Wang, S.; Lyu, Y.; Xu, Y.; Chen, Y.; Zhang, X. Improvement of the thermal conductivity model for turfy soil in view of organic matter content and decomposition degree. *Trans. Chin. Soc. Agric. Eng.* **2024**, *40*, 120–128. [CrossRef]
37. Gao, Y.; Wang, Q.; Liu, Y.; He, J.; Chen, W.; Xing, J.; Sun, M.; Gao, Z.; Wang, Z.; Zhang, M.; et al. Optimal water, nitrogen, and density management increased wheat yield by improving population uniformity. *Agric. Water Manag.* **2025**, *310*, 109362. [CrossRef]
38. Shao, G.; Xu, Y.; Zhou, J.; Tian, P.; Ai, J.; Yang, Y.; Zamanian, K.; Zeng, Z.; Zang, H. Enhanced soil organic carbon stability in rhizosphere through manure application. *Soil Tillage Res.* **2024**, *244*, 106223. [CrossRef]

39. Shaukat, M.; Hoshide, A.K.; Muhammad, S.; Arshad, I.A.; Mushtaq, M.; de Abreu, D.C. Predicting Soil Carbon Sequestration and Harvestable C-Biomass of Rice and Wheat by DNDC Model. *Crops* **2023**, *3*, 220–240. [CrossRef]
40. Zhang, N.; Chen, Z.; Li, Y.; Xu, S.; Miao, S.; Qiao, Y.; Ding, W. Soil organic carbon availability determines the role of crop straws in regulating N2O emissions from maize agroecosystems. *Agric. Ecosyst. Environ.* **2026**, *399*, 110166. [CrossRef]
41. Pandey, A.; Belyaeva, O.; Wijesinghe, T.; Suter, H. Soil nitrate concentrations increase the nitrous oxide to dinitrogen emissions ratio at high soil moisture conditions in intensive dairy pastures. *Biol. Fertil. Soils* **2026**, *62*, 629–637. [CrossRef]
42. Kelley, L.A.; Zhang, Z.; Tamagno, S.; Lundy, M.E.; Mitchell, J.P.; Gaudin, A.C.; Pittelkow, C.M. Changes in soil N_2O emissions and nitrogen use efficiency following long-term soil carbon storage: Evidence from a mesocosm experiment. *Agric. Ecosyst. Environ.* **2024**, *370*, 109054. [CrossRef]
43. Whalen, E.D.; Lounsbury, N.; Geyer, K.; Anthony, M.; Morrison, E.; van Diepen, L.T.A.; Le Moine, J.; Nadelhoffer, K.; vanden Enden, L.; Simpson, M.J.; et al. Root control of fungal communities and soil carbon stocks in a temperate forest. *Soil Biol. Biochem.* **2021**, *161*, 108390. [CrossRef]
44. Queyrel, W.; Van Inghelandt, B.; Colas, F.; Cavan, N.; Granger, S.; Guyot, B.; Reau, R.; Derrouch, D.; Chauvel, B.; Maillot, T.; et al. Combining expert knowledge and models in participatory workshops with farmers to design sustainable weed management strategies. *Agric. Syst.* **2023**, *208*, 103645. [CrossRef]
45. Foldal, C.B.; Kittinger, M.; Haas, E.; Zechmeister-Boltenstern, S. Policy measures effectively reduce soil nitrous oxide emissions with minor trade-offs in crop yield. *Eur. J. Soil Sci.* **2024**, *75*, e13475. [CrossRef]
46. Tong, B.; Kool, D.; Heitman, J.L.; Sauer, T.J.; Gao, Z.; Horton, R. Thermal property values of a central Iowa soil as functions of soil water content and bulk density or of soil air content. *Eur. J. Soil Sci.* **2020**, *71*, 169–178. [CrossRef]
47. Trenz, J.; Memic, E.; Batchelor, W.D.; Graeff-Hönninger, S. Generic optimization approach of soil hydraulic parameters for site-specific model applications. *Precis. Agric.* **2024**, *25*, 654–680. [CrossRef]
48. Gao, J.; Liu, Z.; Wang, P.; Huang, S. Drip irrigation coupled with appropriate N input increased maize (*Zea mays* L.) yield and lodging resistance via optimizing root and stem trait. *Eur. J. Agron.* **2024**, *160*, 127298. [CrossRef]
49. Wang, Y.; He, J.; Gao, Z.; Liu, R.; Hong, Y.; Wang, F.; Mao, X.; Xu, T.; Zhou, L.; Yi, J. Effects of Nitrogen Application Strategies on Yield, Nitrogen Uptake and Leaching in Spring Maize Fields in Northwest China. *Plants* **2025**, *14*, 1067. [CrossRef] [PubMed]
50. Bo, Q.; Ma, T.; Wei, X.; Chen, J.; Zhang, Z.; Li, Y.; Tang, A.; Gao, J.; Zhang, J.; Wei, Y.; et al. Improvement of maize post-silking agronomic traits contributes to high grain yield under N-efficient cultivars. *Field Crops Res.* **2024**, *313*, 109417. [CrossRef]
51. Zhang, Y.; Zhang, G.; Zhai, J.; Cao, Y.; Xu, W.; Ming, B.; Xie, R.; Wang, K.; Li, S.; Xue, J.; et al. Post-Silking Nitrogen Topdressing Optimizes Nitrogen Accumulation and Enhances Yield in Densely Planted Maize. *Agronomy* **2026**, *16*, 26. [CrossRef]

Disclaimer/Publisher's Note: The statements, opinions and data contained in all publications are solely those of the individual author(s) and contributor(s) and not of MDPI and/or the editor(s). MDPI and/or the editor(s) disclaim responsibility for any injury to people or property resulting from any ideas, methods, instructions or products referred to in the content.